

Unitary theory of the deuteron photodisintegration

Hiro Yoshi Tanabe

Institut für Kernphysik, Johannes Gutenberg-Universität, D-6500 Mainz, Federal Republic of Germany

Koichi Ohta

Institute of Physics, University of Tokyo, Komaba, Tokyo 153, Japan

(Received 10 April 1989)

The deuteron photodisintegration in the Δ -resonance region is calculated within a unitary theory of the $NN-N\Delta-\pi NN$ system coupled to the photon. The photoexcitation amplitude of the Δ is deduced from the $M_{1+}(\frac{3}{2})$ pion photoproduction amplitude consistently with its background term and the πN interaction. The $NN-N\Delta$ transition amplitude is obtained from the coupled equations for the $NN-N\Delta-\pi NN$ system. The one-pion-exchange currents as well as the normal single-nucleon current are included. The polarization parameters are reproduced quantitatively, but the cross section is slightly underestimated. Comparison of our results with those of the $NN-N\Delta$ coupled-channel model is made. Effects of relativistic corrections and gauge-invariance constraints are discussed.

I. INTRODUCTION

The $\Delta(1232)$ resonance has now become familiar particle in nuclear physics. Nonetheless, it is a yet harder task to construct a unified model for the NN and $N\Delta$ interactions since the Δ is an unstable particle which ultimately decays into a pion and a nucleon. As a result, the two-body NN and $N\Delta$ channels couple strongly with the three-body πNN channel above the pion-production threshold. This is evidenced by the experimental fact that, in the Δ resonance region, about one-half of the NN total cross section comes from inelastic scattering. Any realistic model for the NN and $N\Delta$ interactions is, therefore, imperatively needed to satisfy the requirement of the three-body unitarity.

During the last decade great efforts have been exerted to build up a unified description of the $NN-N\Delta-\pi NN$ system based on Faddeev's three-body theory. Many authors¹⁻¹¹ have used this approach, the unitary three-body model, as it is often called, to calculate $\pi d \rightarrow \pi d$, $\pi d \rightarrow \pi NN$, $\pi d \rightarrow NN$, $NN \rightarrow NN$, and $NN \rightarrow \pi NN$ reactions. The first two processes are quite well reproduced (except for the backward πd elastic scattering) principally because the quasifree term dominates these reactions. A more intriguing feature of this model is that it can predict pion annihilation and production in qualitatively satisfactory agreement with experiment. The success of the unitary three-body model in describing the $NN-N\Delta$ transition makes it natural to extend the model to electromagnetic processes, $\gamma d \rightarrow pn$, $\pi^0 d$, and πNN .

The deuteron photodisintegration thus far has been studied most intensively in the energy region below the pion-production threshold. The first models for the photodisintegration in the Δ -resonance region appeared in the 1950's,¹² but they did not advance to another stage because of a lack of detailed experimental data to compare with. About ten years ago Laget¹³ resorted to a

diagrammatical approach and carried out systematic studies of the γd reactions. Several calculations¹⁴⁻¹⁶ have appeared after Laget. In these calculations, however, the final-state interaction was treated only approximately or disregarded entirely. Recently Leidemann and Arenhövel¹⁷ applied the $NN-N\Delta$ coupled-channel model to the deuteron photodisintegration. The coupled-channel model, as we shall call it in this paper, incorporates the coupling of the $NN-N\Delta$ system to the πNN channel only through the width of the Δ . Wilhelm, Leidemann, and Arenhövel¹⁸ succeeded in explaining the data qualitatively, especially when they added the relativistic spin-orbit current into their calculation. Preliminary results of an independent attempt based on the coupled-channel model have also appeared in Ref 19.

The coupled-channel model, however, has a conceptual shortcoming; it does not satisfy the three-body unitarity. The purpose of this paper is to extend the unitary three-body model to a description of the deuteron photodisintegration, and to study the validity of the model in its different aspect. We confine ourselves to the photodisintegration, but it is straightforward to apply our model to the pion photoproduction. Among all other things, the essential difference that makes the unitary three-body model distinct from the coupled-channel model is that all the interactions (including off-shell behaviors) are determined by the analyses of the two-body scattering data. This makes the unitary three-body model more consistent dynamically and less flexible practically. In the three-body model the πNN and $\pi N\Delta$ vertex interactions are fixed from πN scattering, while in the model of Leidemann and Arenhövel they could vary these parameters so as to reproduce the NN scattering phase shifts. These observations should be recalled when one compares our results with those of the coupled-channel model.

Another purpose of this paper is to describe the

$\gamma N \rightarrow \pi N$ reaction and the deuteron photodisintegration in a unified way. A formalism which incorporates the electromagnetic interaction into the three-body model has recently been developed by Araki and Afnan.²⁰ As they have pointed out, the $M_{1+}(\frac{3}{2})$ pion-photoproduction amplitude, when embedded in the two-nucleon system, induces two different processes, the Δ -isobar excitation process and the pion-exchange current process. We have to decompose these processes in such a way as to preserve the unitarity constraint. The decomposition of the $M_{1+}(\frac{3}{2})$ amplitude into the resonant and background parts of necessity leads to a modification of the resonant amplitude.²¹ In this paper the $\gamma N \Delta$ coupling constant determined consistently with the background amplitude and the elastic πN amplitude are used to calculate the Δ -isobar current. Furthermore, a dynamical treatment of the pion in the three-body model inevitably produces nonstatic effects on the Δ -isobar current and the pion-exchange currents, which, in the conventional models, have been evaluated in the static limit. Effects of relativistic corrections and gauge-invariance constraints are also investigated.

The outline of this article is as follows. In Sec. II we present our model for the deuteron photodisintegration and describe the connection between the $M_{1+}(\frac{3}{2})$ photoproduction amplitude and the Δ -isobar current. In Sec. III we summarize the necessary formulas for calculating the one-body and two-body current matrix elements. The results and the discussion are given in Sec. IV. Finally, in Sec. V, we present a summary of this work.

II. THE FORMALISM

We describe the system of two nucleons and a pion in terms of the interaction Hamiltonian

$$V = V_d + V_\pi, \quad (2.1)$$

where V_d is the NN interaction in the presence of a spectator pion and V_π is the πN interaction in the presence of a spectator nucleon. Assuming separable two-body interactions for V_d and V_π , the three-body Faddeev equation is reduced to the Faddeev-Lovelace²² equation, as is represented schematically in Fig. 1,

$$T_{\alpha\beta} = \sum_\gamma \left[B_{\alpha\gamma} + \sum_d B_{\alpha d} G_d B_{d\gamma} \right] (\delta_{\gamma\beta} + G_\gamma T_{\gamma\beta}). \quad (2.2)$$

The indices α, β, γ run over two-baryon states, the two baryons being a πN composite and a spectator nucleon, and G is the propagator of the two-body subsystem in the presence of a spectator. The T matrix is driven by the

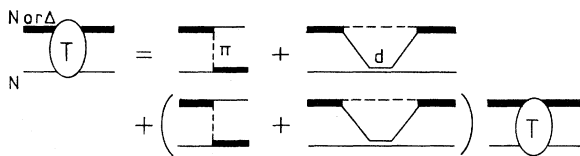


FIG. 1. Faddeev-Lovelace equation for the πNN system.

one-particle exchange Born amplitude B . The index d refers to channels of the NN subsystem and a spectator pion. Equation (2.2) forms a satisfactory basis for the study of pion absorption as developed in Refs. 2-4 and 11.

The P_{11} and P_{33} πN interactions and the 3S_1 - 3D_1 NN interaction are crucially important because each of these amplitudes contains a pole or a resonance. In previous papers,^{10,11} we have calculated the $NN \rightarrow NN$ and $\pi d \rightarrow NN$ reactions including all the S - and P -wave πN interactions and the S -, P -, and 3D_1 -wave NN interactions, but small partial waves did not affect the results of our calculations very much. We shall neglect these partial waves for the sake of simplicity. Consequently, the T matrix elements among NN and $N\Delta$ [the $N(\pi N)$ channels with πN composites in the P_{11} and P_{33} partial waves, respectively], and the driving force has the form

$$B = \begin{bmatrix} f G_{\pi NN}^{(0)} f^\dagger & f G_{\pi NN}^{(0)} f_\Delta^\dagger \\ f_\Delta G_{\pi NN}^{(0)} f^\dagger & f_\Delta G_{\pi NN}^{(0)} f_\Delta^\dagger \end{bmatrix}, \quad (2.3)$$

where the operators f and f_Δ are the $\pi N \rightarrow N$ and $\pi N \rightarrow \Delta$ vertex interactions and $G_{\pi NN}^{(0)}$ is the free πNN propagator. The index d , on the other hand, stands for the πd channel [the $\pi(NN)$ channel with the NN composite in the 3S_1 - 3D_1 partial wave], and the $\pi d \rightarrow NN$ and $\pi d \rightarrow N\Delta$ driving forces are given by

$$B_{NNd} = f G_{\pi NN}^{(0)} f_d^\dagger, \quad (2.4)$$

$$B_{N\Delta d} = f_\Delta G_{\pi NN}^{(0)} f_d^\dagger, \quad (2.5)$$

where f_d is the $d \rightarrow NN$ vertex with one pion being present as a spectator. Its precise definition will be given below. The sum over d in Eq. (2.2) produces the πd -channel coupling. Note that the pion-absorption operator is given by

$$T_{NNd} = \Omega_N^{(-)\dagger} B_{NNd} + \Omega_\Delta^{(-)\dagger} B_{N\Delta d}, \quad (2.6)$$

where

$$\Omega_N^{(-)\dagger} = 1 + T_{NN NN} G_{NN}, \quad (2.7)$$

$$\Omega_\Delta^{(-)\dagger} = T_{NN N\Delta} G_{N\Delta} \quad (2.8)$$

are the distortion operators originating from the final-state interactions. In these equations, G_{NN} and $G_{N\Delta}$ are the NN and $N\Delta$ propagators, respectively. We define $G_{N\Delta}$ in the following way: The $\pi N P_{33}$ scattering amplitude is given by

$$T_{\pi N}(E) = f_\Delta^\dagger G_\Delta(E) f_\Delta, \quad (2.9)$$

where

$$G_\Delta(E) = [E - m_\Delta - \Sigma_\Delta(E)]^{-1} \quad (2.10)$$

is the Δ propagator and

$$\Sigma_\Delta(E) = f_\Delta G_{\pi NN}^{(0)} f_\Delta^\dagger \quad (2.11)$$

is the Δ self-energy. Here m_Δ is the bare mass of the Δ , $G_{\pi NN}^{(0)}$ is the free πN propagator, and E is the bary-centric energy of the πN system. The $G_{N\Delta}$ is equated to $G_\Delta(E)$

with E replaced by the c.m. energy of the πN subsystem.

We now add the electromagnetic interaction V_{em} to the nonradiative interaction Hamiltonian (2.1). We assume that the photon incident on the single nucleon gives rise to three distinct reactions; absorption, Δ excitation, and pion production not mediated by the first two processes, as indicated in Fig. 2. Namely, we assume that V_{em} is given by

$$V_{em} = V_{\gamma}^N + V_{\gamma}^{\Delta} + V_{\pi\gamma}^B, \quad (2.12)$$

where V_{γ}^N is the direct photoabsorption interaction, V_{γ}^{Δ} is the Δ -photoexcitation interaction, and $V_{\pi\gamma}^B$ is the background for the pion photoproduction. From this electromagnetic interaction, the single-nucleon $M_{1+}(\frac{3}{2})$ photoproduction amplitude, as depicted in Fig. 3, is given by^{23,24}

$$T_{\pi\gamma}(E) = V_{\pi\gamma}^B + f_{\Delta}^{\dagger} G_{\Delta}(E) \tilde{V}_{\gamma}^{\Delta} \quad (2.13)$$

in which the first term is the background and the second is the Δ -resonant amplitude modified by the final πN interaction. Namely,

$$\tilde{V}_{\gamma}^{\Delta} = V_{\gamma}^{\Delta} + f_{\Delta} G_{\pi N}^{(0)} V_{\pi\gamma}^B. \quad (2.14)$$

When the electromagnetic interaction (2.12) is applied to a two-nucleon system, it makes a transition to NN , $N\Delta$, or πNN . The photoabsorption operator is calculated from

$$T = \Omega_N^{(-)\dagger} V_{\gamma}^N + \Omega_{\Delta}^{(-)\dagger} V_{\gamma}^{\Delta} + \Omega_N^{(-)\dagger} f G_{\pi NN} V_{\pi\gamma}^B + \Omega_{\Delta}^{(-)\dagger} f_{\Delta} G_{\pi NN} V_{\pi\gamma}^B. \quad (2.15)$$

Here $G_{\pi NN}$ is the πNN propagator

$$G_{\pi NN} = G_{\pi NN}^{(0)} + G_{\pi NN}^{(0)} T_d G_{\pi NN}^{(0)} \quad (2.16)$$

with

$$T_d = V_d + V_d G_{\pi NN}^{(0)} T_d. \quad (2.17)$$

In Eq. (2.15), the first two terms are the processes induced by the one-body nucleon current (the normal current) and the one-body $N \rightarrow \Delta$ transition current (the Δ -isobar current). The nonradiative T matrices obtained from Eq. (2.2) are used to describe the final-state interactions. Equation (2.15) is derived as follows: We decompose the Hilbert space into γNN , NN , $N\Delta$, and πNN . The projection operators onto γNN and πNN are denoted as γ and π , respectively, and the projection operator onto $NN \oplus N\Delta$ is denoted as P . Using the projection operator method, we solve the T matrix for the process $\gamma \rightarrow P$ to order of the electric charge e with the result

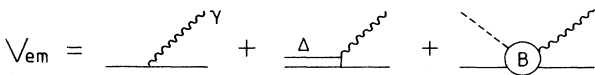


FIG. 2. Electromagnetic interactions for the single nucleon.

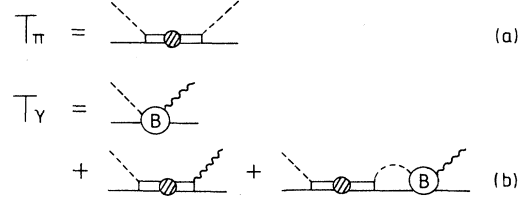


FIG. 3. (a) The $\pi N P_{33}$ scattering amplitude and (b) the $M_{1+}(\frac{3}{2})$ pion-photoproduction amplitude.

$$T_{P\gamma} = V_{P\gamma} + V_{P\pi} G_{\pi NN} V_{\pi\gamma} + T_{PP} G_P V_{P\gamma} + T_{PP} G_P V_{P\pi} G_{\pi NN} V_{\pi\gamma}. \quad (2.18)$$

Within the given interaction (2.12), $V_{\pi\gamma} = V_{\pi\gamma}^B$. We further decompose P into $P_1(NN)$ and $P_2(N\Delta)$ and solve for $T_{P_1\gamma}$,

$$T_{P_1\gamma} = V_{P_1\gamma} + V_{P_1\pi} G_{\pi NN} V_{\pi\gamma}^B + T_{P_1 P_1} G_{P_1} V_{P_1\gamma} + T_{P_1 P_2} G_{P_2} V_{P_2\gamma} + T_{P_1 P_1} G_{P_1} V_{P_1\pi} G_{\pi NN} V_{\pi\gamma}^B + T_{P_1 P_2} G_{P_2} V_{P_2\pi} G_{\pi NN} V_{\pi\gamma}^B. \quad (2.19)$$

Using the notation

$$\begin{aligned} T_{P_1 P_1} &= T_{NN NN}, \\ T_{P_1 P_2} &= T_{NN N\Delta}, \\ G_{P_1} &= G_{NN}, \\ G_{P_2} &= G_{N\Delta}, \end{aligned} \quad (2.20)$$

and $V_{P_1\gamma} = V_{\gamma}^N$, $V_{P_2\gamma} = V_{\gamma}^{\Delta}$, we obtain Eq. (2.15). Within the present model Eq. (2.15) exhausts the photoabsorption process linear in e , thereby the unitarity being ensured to order e . Equation (2.15) is equivalent with Eq. (4.18) in the work of Araki and Afnan.²⁰

Correspondingly to the decomposition (2.16), the $V_{\pi\gamma}^B$ -induced terms in Eq. (2.15) can be split into two parts, the contribution from the free πNN propagator,

$$T_{b.g.} = (\Omega_N^{(-)\dagger} f + \Omega_{\Delta}^{(-)\dagger} f_{\Delta}) G_{\pi NN}^{(0)} V_{\pi\gamma}^B, \quad (2.21)$$

and the correction brought about by T_d ,

$$T_{abs} = (\Omega_N^{(-)\dagger} f + \Omega_{\Delta}^{(-)\dagger} f_{\Delta}) G_{\pi NN}^{(0)} T_d G_{\pi NN}^{(0)} V_{\pi\gamma}^B. \quad (2.22)$$

The T matrix (2.21) contains one-body and two-body processes depending on whether the pion emitted by one nucleon gets reabsorbed by the same nucleon or the other nucleon. The one-body processes can be included into the normal and the Δ -isobar current contributions,

$$T_N = \Omega_N^{(-)\dagger} V_{\gamma}^N + \Omega_N^{(-)\dagger} (f G_{\pi NN}^{(0)} V_{\pi\gamma}^B)_{\text{one body}}, \quad (2.23)$$

$$T_{\Delta} = \Omega_{\Delta}^{(-)\dagger} V_{\gamma}^{\Delta} + \Omega_{\Delta}^{(-)\dagger} (f_{\Delta} G_{\pi NN}^{(0)} V_{\pi\gamma}^B)_{\text{one body}}. \quad (2.24)$$

The two-body processes, on the other hand, are triggered by the two-body $NN \rightarrow NN$ operator

$$V_{\gamma}^{\text{OPE}} = (f G_{\pi NN}^{(0)} V_{\pi\gamma}^B)_{\text{two body}}, \quad (2.25)$$

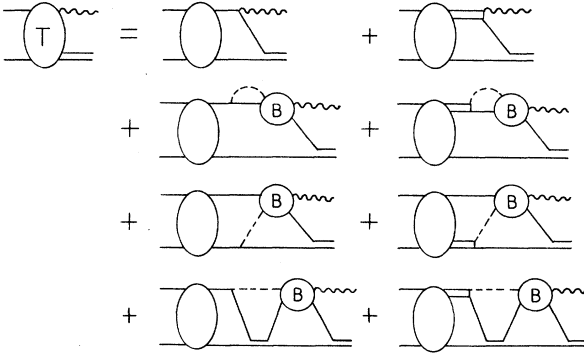


FIG. 4. Photoabsorption operator for the two-nucleon system.

and the two-body $NN \rightarrow N\Delta$ operator

$$V_{\gamma}^{\Delta\text{-OPE}} = (f_{\Delta} G_{\pi NN}^{(0)} V_{\pi\gamma}^B)_{\text{two body}} \quad (2.26)$$

Consequently Eq. (2.15) becomes the sum, as indicated in Fig. 4,

$$T = T_N + T_{\Delta} + T_{N\text{-exc}} + T_{\Delta\text{-exc}} + T_{\text{abs}}, \quad (2.27)$$

where

$$T_{N\text{-exc}} = \Omega_N^{(-)\dagger} V_{\gamma}^{\text{OPE}}, \quad (2.28)$$

$$T_{\Delta\text{-exc}} = \Omega_{\Delta}^{(-)\dagger} V_{\gamma}^{\Delta\text{-OPE}}. \quad (2.29)$$

The Δ -isobar current contribution, Eq. (2.24), can be related to the $M_{1+}(\frac{3}{2})$ amplitude as follows: When one noninteracting nucleon is added, Eq. (2.14) becomes

$$\tilde{V}_{\gamma}^{\Delta} = V_{\gamma}^{\Delta} + (f_{\Delta} G_{\pi NN}^{(0)} V_{\pi\gamma}^B)_{\text{one body}}. \quad (2.30)$$

The Δ -isobar current contribution turns out to be

$$T_{\Delta} = \Omega_{\Delta}^{(-)\dagger} \tilde{V}_{\gamma}^{\Delta}. \quad (2.31)$$

Note that only the Δ -mediated part of the $M_{1+}(\frac{3}{2})$ amplitude is responsible for the Δ -isobar current and that the background is subtracted from the full $M_{1+}(\frac{3}{2})$ amplitude. Note also that the Δ -isobar current is subject to the full nonstatic treatment. This makes our calculation distinct from the traditional approach based on the diagrammatical expansion of the current operators. The background also affects the normal-current contribution as

$$\tilde{V}_{\gamma}^N = V_{\gamma}^N + (fG_{\pi NN}^{(0)} V_{\pi\gamma}^B)_{\text{one body}} \quad (2.32)$$

which leads to the renormalization of the physical quantities of the nucleon, such as mass and magnetic moment, but since we use the observed values for the single-nucleon interaction, inclusion of the dressing of the normal current would result in double counting.

To understand the meaning of Eq. (2.22), we consider a separable NN interaction in the deuteron channel,

$$V_d = g\lambda g^{\dagger}. \quad (2.33)$$

The NN scattering amplitude is given by

$$T_d = g[\lambda^{-1} - \Sigma_d(E)]^{-1} g^{\dagger}, \quad (2.34)$$

where

$$\Sigma_d(E) = g^{\dagger} G_{NN}^{(0)} g \quad (2.35)$$

and $G_{NN}^{(0)}$ is the free NN propagator. Since the scattering amplitude possesses a pole at the deuteron mass m_d , one sees that

$$[\lambda^{-1} - \Sigma_d(E)]^{-1} \cong C^2 / (E - m_d), \quad (2.36)$$

where

$$C^{-2} = - \left. \frac{d\Sigma_d(E)}{dE} \right|_{E=m_d}. \quad (2.37)$$

The deuteron wave function is given by

$$\phi = CG_{NN}^{(0)} g \quad (2.38)$$

which is normalized to unity at $E = m_d$.

We now add a noninteracting pion as a spectator. The NN amplitude becomes

$$T_d = f_d G_d f_d^{\dagger}, \quad (2.39)$$

where G_d is the free πd propagator and

$$f_d = Cg \quad (2.40)$$

is the $d \rightarrow NN$ vertex function. Furthermore, from Eq. (2.38), the πd wave function becomes

$$\psi_d = G_{\pi NN}^{(0)} f_d, \quad (2.41)$$

$$\psi_d^{\dagger} = f_d^{\dagger} G_{\pi NN}^{(0)}. \quad (2.42)$$

Inserting Eq. (2.39) into Eq. (2.22) leads to

$$T_{\text{abs}} = T_{NNd} G_d \psi_d^{\dagger} V_{\pi\gamma}^B, \quad (2.43)$$

where the pion-absorption amplitude, Eq. (2.6), takes the form

$$T_{NNd} = (\Omega_N^{(-)\dagger} f + \Omega_{\Delta}^{(-)\dagger} f_{\Delta}) \psi_d. \quad (2.44)$$

Equation (2.43) can be written in the form

$$T_{\text{abs}} = \Omega_d^{(-)\dagger} V_{\pi\gamma}^B \quad (2.45)$$

with

$$\Omega_d^{(-)\dagger} = (\Omega_N^{(-)\dagger} f + \Omega_{\Delta}^{(-)\dagger} f_{\Delta}) \psi_d G_d \psi_d^{\dagger}. \quad (2.46)$$

Thus, it turned out that (2.22) describes the quasielastic pion photoproduction followed by the pion absorption. We shall call this the pion-reabsorption term. Equation (2.45) holds independently of the particular model for the NN interaction that we have used.

Each of the five contributions in Eq. (2.27) has the form of the impulse term distorted by the final-state interaction,

$$T = -\Omega^{(-)\dagger} \int d\mathbf{x} \hat{J}_{\mu}(\mathbf{x}) A_{\mu}(\mathbf{x}), \quad (2.47)$$

with A_{μ} being the electromagnetic potential. The four-current $\hat{J}_{\mu} = (\hat{\mathbf{J}}, i\hat{\rho})$ consists of the components corresponding to V_{γ}^N , V_{γ}^{Δ} , V_{γ}^{OPE} , $V_{\gamma}^{\Delta\text{-OPE}}$, and $V_{\pi\gamma}^B$,

$$\hat{J}_\mu = \hat{J}_\mu^N + \hat{J}_\mu^\Delta + \hat{J}_\mu^{\text{OPE}} + \hat{J}_\mu^{\Delta\text{-OPE}} + \hat{J}_\mu^B, \quad (2.48)$$

and

$$\Omega^{(-)\dagger} = \Omega_N^{(-)\dagger} + \Omega_\Delta^{(-)\dagger} + \Omega_d^{(-)\dagger}. \quad (2.49)$$

In this section we have simplified the argument by employing the Δ -isobar dominated model for πN elastic scattering. In a previous paper,²⁴ we introduced the elastic background and constructed a dynamically consistent model for the pion photoproduction. We use this model to determine the $\gamma N \Delta$ coupling constant under the constraint of unitarity and calculate the Δ -isobar current. The $\pi N P_{11}$ interaction is also described by a two-potential model.^{2-4,10} Since we take these interactions to be separable, appropriate modifications of the formulas are made straightforwardly by introducing matrix notations

$$f = \begin{pmatrix} f^1 \\ f^2 \end{pmatrix}, \quad f_\Delta = \begin{pmatrix} f_\Delta^1 \\ f_\Delta^2 \end{pmatrix}, \quad (2.50)$$

in which the index 1 is for the pole terms we have discussed in this section while the index 2 is for the nonpole background terms. The effect of such a complication is to double the channel quantum numbers. The operator T_{NNd} becomes a 2×2 matrix. The physical amplitude can be extracted from this by multiplying the renormalization factor Z as is described in our previous paper.¹⁰

We conclude this section by devoting a brief discussion to the gauge invariance. The total Hamiltonian

$$H = H_0 + V_d + V_\pi + V_\gamma^N + V_\gamma^\Delta + V_{\pi\gamma}^B \quad (2.51)$$

should be invariant under a local gauge transformation. The free Hamiltonian H_0 is the sum of the kinetic-energy operators of π , N , and Δ . The single-nucleon electromagnetic interaction V_γ^N should emerge consistently with the nucleon kinetic-energy operator in H_0 . We shall describe

the normal current in Sec. III A. The interaction current associated with V_d is not involved in the γd reactions. The gauge-invariance requirement imposed on the πN interaction V_π produces a $\gamma N \rightarrow \pi N$ interaction from f^\dagger and a $\gamma N \rightarrow \pi \Delta$ interaction from f_Δ^\dagger . The $\gamma N \rightarrow \pi N$ interaction is included in $V_{\pi\gamma}^B$ but the $\gamma N \rightarrow \pi \Delta$ interaction is not present in (2.51) since we do not consider the three-body state $\pi N \Delta$ as a coupled channel. The effect of the $\gamma N \rightarrow \pi \Delta$ interaction will be taken into account as one of the $NN \rightarrow N \Delta$ pion-exchange currents, as described in Sec. III C. We do not consider the internal bremsstrahlung of the Δ since it does not contribute to the γd reactions unless the $\Delta \Delta$ component of the deuteron wave function is present.

III. CURRENT MATRIX ELEMENTS

The transition amplitude for the deuteron photodisintegration is written as

$$\langle \mathbf{p} | T | \mathbf{k}, \lambda, \phi \rangle = - \frac{\epsilon_\mu^\lambda}{\sqrt{2\omega}} \langle \mathbf{p} | \Omega^{(-)\dagger} \hat{J}_\mu(\mathbf{k}) | \phi \rangle, \quad (3.1)$$

where \mathbf{p} is the relative momentum of the pn system, \mathbf{k} is the photon momentum, ϵ_μ^λ is the polarization vector with λ being the photon helicity, and $\omega = k$ is the energy of the incident photon. We use the c.m. system as a reference frame. Inserting the intermediate NN , $N\Delta$, and πd states, we obtain

$$\begin{aligned} \langle \mathbf{p} | T | \mathbf{k}, \lambda, \phi \rangle \\ = - \frac{\epsilon_\mu^\lambda}{\sqrt{2\omega}} \cdot \int \frac{d\mathbf{p}'}{(2\pi)^3} \langle \mathbf{p} | \Omega^{(-)\dagger} | \mathbf{p}' \rangle \langle \mathbf{p}' | \hat{J}_\mu(\mathbf{k}) | \phi \rangle. \end{aligned} \quad (3.2)$$

For the purpose of practical calculations, we expand the transition amplitude into partial waves in terms of the reduced matrix elements

$$\begin{aligned} J_{Ll_0}(lsJ) &= \langle p, lsJ | \Omega^{(-)\dagger} \hat{J} | k, Ll_0J \rangle \\ &= (2\pi)^{-3} \sum_{l's'} \int_0^\infty p'^2 dp' \langle p, lsJ | \Omega^{(-)\dagger} | p', l's'J \rangle \langle p', l's'J | \hat{J} | k, Ll_0J \rangle, \end{aligned} \quad (3.3)$$

$$\begin{aligned} \rho_L(lsJ) &= \langle p, lsJ | \Omega^{(-)\dagger} \hat{\rho} | k, LJ \rangle \\ &= (2\pi)^{-3} \sum_{l's'} \int_0^\infty p'^2 dp' \langle p, lsJ | \Omega^{(-)\dagger} | p', l's'J \rangle \langle p', l's'J | \hat{\rho} | k, LJ \rangle, \end{aligned} \quad (3.4)$$

where l and s are the orbital angular momentum and the total spin of the pn system, respectively, and J is the total angular momentum. The photon is assigned the orbital angular momentum l_0 and the total angular momentum L . The sums are over intermediate two-body states NN , $N\Delta$, and πd . The minimal-relativity prescription²⁵ is applied to the final-state interactions.

In terms of the reduced matrix elements (3.3) and (3.4), the electric, magnetic, and Coulomb multipoles are written as

$$E_L(lsJ) = \sqrt{L+1} J_{LL-1}(lsJ) + \sqrt{L} J_{LL+1}(lsJ), \quad (3.5a)$$

$$M_L(lsJ) = \sqrt{2L+1} J_{LL}(lsJ), \quad (3.5b)$$

$$C_L(lsJ) = \sqrt{2L+1} \rho_L(lsJ). \quad (3.5c)$$

The longitudinal multipole is not independent. Thanks to the gauge invariance, we can use the continuity equation and write the longitudinal multipole in terms of the Coulomb multipole,

$$\begin{aligned} L_L(lsJ) &= \sqrt{L} J_{LL-1}(lsJ) - \sqrt{L+1} J_{LL+1}(lsJ) \\ &= \frac{\omega}{k} C_L(lsJ). \end{aligned} \quad (3.5d)$$

It is well known that the electric multipole, which is strongly influenced by meson-exchange currents, can be reliably calculated by exploiting the continuity-equation constraint (3.5d). The way to implement the constraint is not unique, however. We follow Eisenberg and Greiner,²⁶ and substitute Eq. (3.5d) into Eq. (3.5a) with the result

$$E_L(lsJ) = \left[\frac{L+1}{L} \right]^{1/2} \frac{\omega}{k} C_L(lsJ) + \frac{2L+1}{\sqrt{L}} J_{LL+1}(lsJ). \quad (3.6)$$

In the long-wavelength limit the second part and the meson-exchange effect on the Coulomb multipole vanish. Consequently, the electric multipole is determined model independently once the continuity equation is used. This fact is known as Sigert's theorem. The model independence of the electric multipole persists at moderate value of k , and hence it is a common practice to impose the continuity-equation constraint even if theoretical models do not obey rigorously the current-conservation law.

A. Normal current

We define the single-nucleon current matrix element by

$$\langle -\mathbf{p} | \hat{J}_\mu^N | \mathbf{k}\lambda, n \rangle = (2\pi)^3 \delta(\mathbf{n} + \mathbf{k} + \mathbf{p}) J_\mu(\mathbf{k}). \quad (3.7)$$

Since the spectator nucleon carries momentum \mathbf{p} , the nucleon interacting with the photon has momenta $\mathbf{n} = -\mathbf{p} - \mathbf{k}$ and $-\mathbf{p}$, and energies

$$E_n = [(\mathbf{p} + \mathbf{k})^2 + m^2]^{1/2}, \quad (3.8a)$$

$$E_p = (\mathbf{p}^2 + m^2)^{1/2}, \quad (3.8b)$$

respectively, before and after the interaction. The kinematics is shown in Fig. 5. The most general form of $J_\mu(\mathbf{k})$ is

$$\mathbf{J}(\mathbf{k}) = g_1 \mathbf{p} + g_2 \mathbf{k} + ig_3 \boldsymbol{\sigma} \times \mathbf{p} + ig_4 \boldsymbol{\sigma} \times \mathbf{k} + ig_5 \boldsymbol{\sigma} \cdot \mathbf{p} \times \mathbf{k} + ig_6 \boldsymbol{\sigma} \cdot \mathbf{k} \times \mathbf{p}, \quad (3.9)$$

$$\rho(\mathbf{k}) = h_1 + ih_2 \boldsymbol{\sigma} \cdot \mathbf{p} \times \mathbf{k}. \quad (3.10)$$

The form factors are functions of p , k , and $\hat{\mathbf{p}} \cdot \hat{\mathbf{k}}$. Two more vectors

$$\mathbf{p} \cdot \mathbf{p} \times \mathbf{k} = \mathbf{p} \cdot \mathbf{k} \times \mathbf{p} - \mathbf{p}^2 \boldsymbol{\sigma} \times \mathbf{k} + \boldsymbol{\sigma} \cdot \mathbf{p} \times \mathbf{k}, \quad (3.11a)$$

$$\mathbf{k} \cdot \mathbf{p} \times \mathbf{k} = \mathbf{k}^2 \boldsymbol{\sigma} \times \mathbf{p} - \mathbf{p} \cdot \mathbf{k} \times \mathbf{k} + \boldsymbol{\sigma} \cdot \mathbf{k} \times \mathbf{p} \quad (3.11b)$$

do not define independent form factors.

The direct photoabsorption interaction is derived from the Dirac Hamiltonian in the electromagnetic external field. The current matrix element is subject to unitary-

$$N = \frac{1}{\sqrt{2E_p(E_p+m)2E_n(E_n+m)}}, \quad (3.15a)$$

$$L = -i \frac{E_p - E_n}{E_p + E_n} \frac{(E_p + E_n + 2m)^2 + 4E_p E_n}{(E_p + E_n)(E_p + E_n + 2m) + 2\sqrt{2E_p(E_p+m)2E_n(E_n+m)}}, \quad (3.15b)$$

$$G = F_1 + F_2(E_p + E_n + 2m). \quad (3.15c)$$

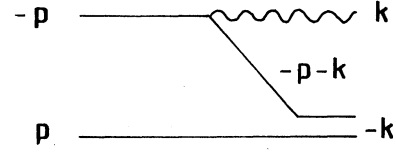


FIG. 5. Momentum assignment for the impulse term.

equivalence ambiguity, i.e.,

$$J_\mu(\mathbf{k}) = i\bar{u}(-\mathbf{p})(F_1\gamma_\mu - F_2\sigma_{\mu\nu}k_\nu)u(-\mathbf{p}-\mathbf{k}) + i(E_p - E_n - \omega)S_\mu(\mathbf{k}), \quad (3.12)$$

where the first term is the matrix element of the Dirac electromagnetic current (F_1 and F_2 are the Dirac form factors,

$$G_E = F_1 - (k_\mu^2/2m)F_2$$

and

$$G_M = F_1 + 2mF_2$$

are the Sachs form factors, $k_\mu^2 = \mathbf{k}^2 - \omega^2$, and m is the nucleon mass) and $S_\mu(\mathbf{k})$ is the matrix element of the generator of a time-dependent unitary transformation S ,

$$\langle -\mathbf{p} | S | \mathbf{k}\lambda, \mathbf{n} \rangle = -(2\pi)^3 \delta(\mathbf{n} + \mathbf{k} + \mathbf{p}) \frac{\epsilon_\mu^\lambda}{\sqrt{2\omega}} S_\mu(\mathbf{k}). \quad (3.13)$$

The generator S is completely arbitrary. Such a nonuniqueness, sometimes called Barnhill's ambiguity in the context of the pion-nucleon vertex,²⁷ can be exploited to make the electromagnetic interaction explicitly gauge invariant consistently with the diagonalized nucleon-energy operator $\beta(-\nabla^2 + m^2)^{1/2}$ rather than with the original Dirac Hamiltonian $-i\boldsymbol{\alpha} \cdot \nabla + \beta m$.²⁸⁻³⁰ The explicit form for S has been obtained²⁹ and the form factors have been given by

$$g_1 = N(-iF_1\omega L + F_2k_\mu^2) - \frac{2F_1}{E_p + E_n}, \quad (3.14a)$$

$$g_2 = \frac{1}{2}g_1 - \frac{1}{2}N[G\omega + F_2(2\mathbf{p} \cdot \mathbf{k} + \mathbf{k}^2)], \quad (3.14b)$$

$$g_3 = NG\omega, \quad (3.14c)$$

$$g_4 = \frac{1}{2}g_3 + \frac{1}{2}N[G(E_p + E_n) + 2mG_E], \quad (3.14d)$$

$$g_5 = 2g_6 = -2NF_2, \quad (3.14e)$$

$$h_1 = \frac{1}{2}N[F_1(E_p + E_n)(E_p + E_n + 2m) - G\mathbf{k}^2 - F_2\omega(2\mathbf{p} \cdot \mathbf{k} + \mathbf{k}^2)], \quad (3.14f)$$

$$h_2 = NG, \quad (3.14g)$$

where

$$N = \frac{1}{\sqrt{2E_p(E_p+m)2E_n(E_n+m)}}, \quad (3.15a)$$

$$L = -i \frac{E_p - E_n}{E_p + E_n} \frac{(E_p + E_n + 2m)^2 + 4E_p E_n}{(E_p + E_n)(E_p + E_n + 2m) + 2\sqrt{2E_p(E_p+m)2E_n(E_n+m)}}, \quad (3.15b)$$

$$G = F_1 + F_2(E_p + E_n + 2m). \quad (3.15c)$$

Because of the identities

$$g_3 - \omega h_2 = 0, \quad (3.16)$$

$$\mathbf{p} \cdot \mathbf{k} g_1 + \mathbf{k}^2 g_2 - \omega h_1 = F_1(E_p - E_n - \omega), \quad (3.17)$$

the four divergence of the current turns out to be³¹

$$\mathbf{k} \cdot \mathbf{J}(\mathbf{k}) - \omega \rho(\mathbf{k}) = F_1(E_p - E_n - \omega). \quad (3.18)$$

The normal current is not conserved by itself. The use of the continuity equation amounts to including a part of the meson-exchange currents, thus bringing us a more reliable estimate of the electric multipole, at least at low energies.

It is straightforward to expand the full relativistic form factors in a power series of m^{-1} using

$$N = \frac{1}{4m^2} + O(m^{-4}), \quad (3.19a)$$

$$L = O(m^{-2}), \quad (3.19b)$$

$$G = 2G_M - G_E + O(m^{-2}), \quad (3.19c)$$

and obtain

$$g_1 \cong -\frac{G_E}{m}, \quad (3.20a)$$

$$g_2 \cong -\frac{G_E}{2m} - \frac{2G_M - G_E}{8m^2} \omega, \quad (3.20b)$$

$$g_3 \cong \frac{2G_M - G_E}{4m^2} \omega, \quad (3.20c)$$

$$g_4 \cong \frac{G_M}{2m} + \frac{2G_M - G_E}{8m^2} \omega, \quad (3.20d)$$

$$g_5 \cong 0, \quad (3.20e)$$

$$g_6 \cong 0, \quad (3.20f)$$

$$h_1 \cong G_E - \frac{2G_M - G_E}{8m^2} k^2, \quad (3.20g)$$

$$h_2 \cong \frac{2G_M - G_E}{4m^2}, \quad (3.20h)$$

in precise agreement with the result of the successive Foldy-Wouthuysen³² transformations to order m^{-2} . Note that for the real photon, $G_E = F_1$. The g_2 term is for the longitudinal current which does not contribute to the real photon processes. When we use the continuity equation, we replace a part of the electric multipole with the Coulomb multipole. This necessitates us to retain the convection current in g_2 . The Darwin-Foldy terms can be dropped from g_2 and h_1 . In fact, the g_2 and h_1 terms contribute to the electric multipole in the combination $(\omega/k)h_1 - kg_2$ so that the Darwin-Foldy terms cancel each other between g_2 and h_1 .

For the partial-wave expansion, we choose the direction of the photon momentum as the quantization axis and rewrite Eqs. (3.9) and (3.10) in terms of tensors

$$J_\lambda(\mathbf{k}) = g_1 C_{1\lambda}(\hat{\mathbf{p}}) + g_2 \delta_{\lambda 0} + g_3 [C_1(\hat{\mathbf{p}}) \times \sigma]_{1\lambda} - g_4 \lambda \sigma_\lambda - g_5 \lambda [C_2(\hat{\mathbf{p}}) \times \sigma]_{1\lambda}, \quad (3.21)$$

$$\rho(\mathbf{k}) = h_1 + h_2 [C_1(\hat{\mathbf{p}}) \times \sigma]_{10}, \quad (3.22)$$

where the form factors are redefined as

$$g_1 \rightarrow pg_1, \quad (3.23a)$$

$$g_2 \rightarrow kg_2, \quad (3.23b)$$

$$g_3 \rightarrow -\sqrt{2}p(g_3 - k^2 g_6), \quad (3.23c)$$

$$g_4 \rightarrow -k(g_4 + \frac{1}{3}p^2 g_5 + \mathbf{p} \cdot \mathbf{k} g_6), \quad (3.23d)$$

$$g_5 \rightarrow \frac{\sqrt{10}}{3} kp^2 g_5, \quad (3.23e)$$

$$h_1 \rightarrow h_1, \quad (3.23f)$$

$$h_2 \rightarrow -\sqrt{2}kph_2. \quad (3.23g)$$

The product of the one-body current matrix element and the deuteron wave function yields the impulse approximation

$$J_{Ll_0}(lsJ) = \langle lsJ || J(\mathbf{k}) \phi(\mathbf{Q}) || Ll_0J \rangle, \quad (3.24)$$

$$p_L(lSJ) = \langle lsJ || \rho(\mathbf{k}) \phi(\mathbf{Q}) || LJ \rangle. \quad (3.25)$$

The deuteron wave function in momentum space, $\phi(\mathbf{Q}) = \langle \mathbf{Q} | \phi \rangle$, is calculated in its rest frame as a function of the pn relative momentum

$$Q_x = p_x, \quad Q_y = p_y, \quad Q_z = \gamma(p_z + vE_p), \quad (3.26)$$

where $v = k/E_d$, $\gamma = E_d/m_d$, and $E_d = (k^2 + m_d^2)^{1/2}$ is the deuteron energy. In the nonrelativistic limit, $Q_z = p_z + \frac{1}{2}k$. The relativistic corrections arise from terms beyond order m^{-1} in the current and the Lorentz boost in the pn relative momentum. The Wigner spin rotation is neglected since its effect is found to be small.³³ The explicit expressions for the multipoles are given in Appendix A.

B. Δ -isobar current

The N - Δ electromagnetic transition is overwhelmingly predominated by the magnetic dipole. The Δ -isobar current contribution is calculated as the two-step process, the Δ excitation followed by the $N\Delta \rightarrow NN$ transition, as described in Sec. II. The current matrix element becomes

$$\langle -\mathbf{p} | \hat{J}_\mu^\Delta | \mathbf{k}\lambda, n \rangle = (2\pi)^3 \delta(\mathbf{n} + \mathbf{p} + \mathbf{k}) J_\mu^\Delta(\mathbf{k}), \quad (3.27)$$

where

$$\mathbf{J}^\Delta(\mathbf{k}) = iF_\Delta \mathbf{S} \times \left[\mathbf{k} + \frac{E_\Delta - E_n}{E_\Delta} \mathbf{p} \right], \quad (3.28)$$

$$\rho^\Delta(\mathbf{k}) = iF_\Delta \frac{1}{E_\Delta} \mathbf{S} \cdot \mathbf{p} \times \mathbf{k}. \quad (3.29)$$

In these equations, \mathbf{S} is the transition spin operator, E_Δ is the energy of the Δ , and

$$F_\Delta = \sqrt{2/3} \frac{f_{\gamma N\Delta}}{2m} \quad (3.30)$$

is the $\gamma N\Delta$ coupling constant multiplied by the isospin Clebsch-Gordan coefficient for the Δ excitation. The

four divergence of the transition current becomes

$$\mathbf{k} \cdot \mathbf{J}^\Delta(\mathbf{k}) - \omega \rho^\Delta(\mathbf{k}) = (E_\Delta - E_n - \omega) \rho^\Delta(\mathbf{k}). \quad (3.31)$$

Equations (3.28) and (3.29) are readily rewritten in terms of tensors

$$J_\lambda^\Delta(\mathbf{k}) = g_3^\Delta [C_1(\hat{p}) \times S]_{1\lambda} - g_4^\Delta \lambda S_\lambda, \quad (3.32)$$

$$\rho^\Delta(\mathbf{k}) = h_2^\Delta [C_1(\hat{p}) \times S]_{10}, \quad (3.33)$$

where

$$g_3^\Delta = -\sqrt{2} p F_\Delta \frac{E_\Delta - E_n}{E_\Delta}, \quad (3.34a)$$

$$g_4^\Delta = -k F_\Delta, \quad (3.34b)$$

$$h_2^\Delta = -\sqrt{2} p F_\Delta \frac{k}{E_\Delta}. \quad (3.34c)$$

The $\gamma N \Delta$ coupling constant is deduced by fitting the $M_{1+}(\frac{3}{2})$ photoproduction amplitude (2.13) to the experimental data. The extraction of F_Δ is complicated by the presence of the background and the final πN rescattering. Equation (2.14) defines the effective $\gamma N \Delta$ vertex function $\bar{F}_\Delta(E)$. We approximate the background of the $M_{1+}(\frac{3}{2})$ amplitude by the sum of the three Born amplitudes; the contact amplitude,³⁴ the pionic amplitude, and the one-nucleon exchange amplitude. The πNN and $\gamma \pi NN$ vertices in the Born amplitude are multiplied by a common form factor. Once F_Δ is determined, $\bar{F}_\Delta(E)$ is calculated as a function of the c.m. energy of the πN subsystem. With $\bar{F}_\Delta(E)$ in place of F_Δ in Eq. (3.28), the Δ -isobar current contribution (2.31) is evaluated.

C. One-pion-exchange currents

The photodisintegration amplitude is given by

$$\langle \mathbf{p} | \hat{\mathbf{J}}^{\text{OPE}} | \mathbf{k} \lambda, \phi \rangle = \int \frac{d\mathbf{p}'}{(2\pi)^3} \mathbf{J}_{\text{OPE}}(\mathbf{k}) \phi(\mathbf{p}' + \frac{1}{2}\mathbf{k}), \quad (3.35)$$

with the matrix element of the one-pion-exchange current

$$\mathbf{J}_{\text{OPE}}(\mathbf{k}) = i f(\kappa) \tau_2^a \sigma_2 \cdot \kappa G_{\pi NN}^{(0)}(\mathbf{p}, \mathbf{p}') \mathbf{J}_B^a(\mathbf{k}), \quad (3.36)$$

where κ is the πN relative momentum, $f(\kappa)$ is the πNN vertex function, and a is the pion isospin index. The current matrix element of the background is defined by

$$\langle \mathbf{p}, \mathbf{q} a | \hat{\mathbf{J}}^B(\mathbf{k}) | -\mathbf{p}' - \mathbf{k} \rangle = (2\pi)^3 \delta(\mathbf{q} + \mathbf{p} + \mathbf{p}') \mathbf{J}_B^a(\mathbf{k}), \quad (3.37)$$

with $\mathbf{q} = -\mathbf{p} - \mathbf{p}'$ being the pion momentum. The pion wave-function normalization $(2\omega_q)^{-1}$ is included in the πNN propagator $G_{\pi NN}^{(0)}(\mathbf{p}, \mathbf{p}')$ [$\omega_q = (\mathbf{q}^2 + \mu^2)^{1/2}$ is the pion energy and μ is the pion mass]. The backward-going pion propagator is approximated by the static one and is added to the πNN propagator so that Eq. (3.36) has the correct static limit. The pn relative momentum in the deuteron is considered in the nonrelativistic limit. The momenta are defined as in Fig. 6. The diagram with nucleons 1 and 2 interchanged should be added unless it coincides with Eq. (3.36).

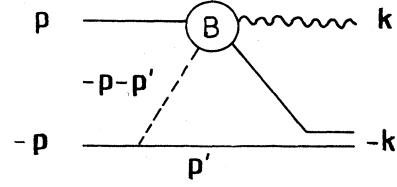


FIG. 6. Momentum assignment for the exchange-current processes.

First we evaluate Eq. (3.36) using the static approximation

$$G_{\pi NN}^{(0)}(\mathbf{p}, \mathbf{p}') \cong -1/\omega_q^2, \quad (3.38a)$$

$$\kappa \cong \mathbf{q}. \quad (3.38b)$$

Furthermore, we again approximate the background by the contact and pionic Born terms. Using the notation $\mathbf{q}_1 = \mathbf{q} - \mathbf{k}$, $\mathbf{q}_2 = \mathbf{q}$, $\omega_1 = \omega_{\mathbf{q}-\mathbf{k}}$, and $\omega_2 = \omega_{\mathbf{q}}$,

$$\begin{aligned} \mathbf{J}_B^a(\mathbf{k}) \cong & -\varepsilon^{zab} \tau_1^b \sigma_2 f(q_2) \\ & + \varepsilon^{zab} \tau_1^b f(q_1) \frac{(\mathbf{q}_1 + \mathbf{q}_2) \sigma_1 \cdot \mathbf{q}_1}{\omega_1^2}. \end{aligned} \quad (3.38c)$$

We do not include the one-nucleon exchange Born term which produces the recoil-current contribution in Fig. 7(b), its leading part being canceled, in the static limit, by the deuteron wave-function renormalization. We find that the one-pion-exchange current is the sum of the contact current, Fig. 7(a), and the pionic current, Fig. 7(c). The contact interaction, the first term in (3.38c), and the contact interaction on nucleon 2 yield the exchange current

$$\begin{aligned} \mathbf{J}_{\text{contact}}(\mathbf{k}) = & -i(\tau_1 \times \tau_2)^z \left[f(q_1)^2 \frac{\sigma_2 \sigma_1 \cdot \mathbf{q}_1}{\omega_1^2} \right. \\ & \left. + f(q_2)^2 \frac{\sigma_1 \sigma_2 \cdot \mathbf{q}_2}{\omega_2^2} \right]. \end{aligned} \quad (3.39a)$$

The pionic interaction, the second term in (3.38c), produces the exchange current

$$\begin{aligned} \mathbf{J}_{\text{pionic}}(\mathbf{k}) = & i(\tau_1 \times \tau_2)^z \xi(q_1, q_2) f(q_1) f(q_2) \\ & \times \frac{(\mathbf{q}_1 + \mathbf{q}_2) \sigma_1 \cdot \mathbf{q}_1 \sigma_2 \cdot \mathbf{q}_2}{\omega_1^2 \omega_2^2}. \end{aligned} \quad (3.39b)$$

It is well known that the insertion of form factors into the meson-nucleon vertices leads to a violation of gauge invariance. The reason for this is that the extra additional current is unavoidably associated with the inserted ha-

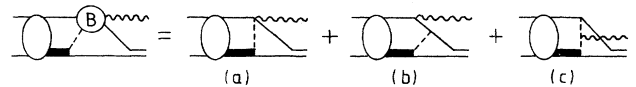


FIG. 7. Contribution of $V_{\pi\gamma}^B$ to the one-pion-exchange current.

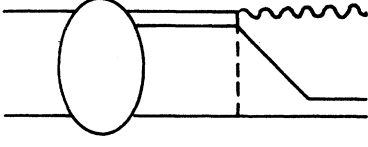


FIG. 8. Δ one-pion-exchange current from the $\gamma N \rightarrow \pi \Delta$ contact interaction.

dronic form factor.³⁵ We follow the prescription developed in Ref. 36 and supplement the additional current

$$\delta J_B^a(\mathbf{k}) = -\epsilon^{zab} \tau_1^b \sigma_1 \cdot \mathbf{q}_1 \frac{\mathbf{q}_1 + \mathbf{q}_2}{q_2^2 - q_1^2} [f(q_2) - f(q_1)]. \quad (3.40)$$

The factor in the pionic current

$$\xi(q_1, q_2) = 1 - \frac{f(q_2) - f(q_1)}{q_2^2 - q_1^2} \left[\frac{\omega_1^2}{f(q_1)} + \frac{\omega_2^2}{f(q_2)} \right], \quad (3.41)$$

accounts for the current (3.40) (and the one on nucleon 2), and guarantees that the one-pion-exchange current obeys the gauge-invariance condition

$$\mathbf{k} \cdot \mathbf{J}_{\text{OPE}}(\mathbf{k}) = [V_{\text{OPE}}(\mathbf{q}_2), \frac{1}{2}(1 + \tau_1^z)] + [V_{\text{OPE}}(\mathbf{q}_1), \frac{1}{2}(1 + \tau_2^z)], \quad (3.42)$$

where

$$V_{\text{OPE}}(\mathbf{q}) = -\tau_1 \cdot \tau_2 f(q)^2 \frac{\sigma_1 \cdot \mathbf{q} \sigma_2 \cdot \mathbf{q}}{\omega_q^2} \quad (3.43)$$

is the one-pion-exchange NN potential. The pionic current corrected by the form-factor effect was obtained by solving the gauge-invariance condition (3.42).^{37,38} The approach of Ref. 36 is to derive it from the minimal-substitution prescription applied to a nonlocal representation of the πNN vertex.

In a quite similar way we can derive the formulas to calculate the one-pion-exchange current for the $NN \rightarrow N\Delta$ transition. Figure 7(b) is the recoil current which vanishes identically owing to the isospin conservation. In addition to the $\gamma N \rightarrow \pi N$ contact interaction, Fig. 7(a), there should exist the $\gamma N \rightarrow \pi \Delta$ contact interaction, Fig. 8. The latter is required because of the presence of the derivative and form factor at the $\pi N \Delta$ vertex. We extend the approach of Ref. 36 and derive the contact current by a minimal replacement in the $\pi N \Delta$ vertex with the result

$$J_\Delta^a(\mathbf{k}) = -\epsilon^{zab} T_2^b S_2 f_\Delta(q_1) - \epsilon^{zab} T_2^b S_2 \cdot \mathbf{q}_2 \frac{\mathbf{q}_1 + \mathbf{q}_2}{q_2^2 - q_1^2} [f_\Delta(q_2) - f_\Delta(q_1)]. \quad (3.44)$$

The Δ -isobar one-pion-exchange current is again the sum of the contact current,

$$J_{\text{contact}}^\Delta(\mathbf{k}) = -i(\tau_1 \times \mathbf{T}_2)^z \times \left[f(q_1) f_\Delta(q_1) \frac{\mathbf{S}_2 \sigma_1 \cdot \mathbf{q}_1}{\omega_1^2} + f(q_2) f_\Delta(q_2) \frac{\sigma_1 \mathbf{S}_2 \cdot \mathbf{q}_2}{\omega_2^2} \right], \quad (3.45a)$$

and the pionic current, Fig. 7(b),

$$J_{\text{pionic}}^\Delta(\mathbf{k}) = i(\tau_1 \times \mathbf{T}_2)^z \xi_\Delta(q_1, q_2) f(q_1) f_\Delta(q_2) \times \frac{(\mathbf{q}_1 + \mathbf{q}_2) \sigma_1 \cdot \mathbf{q}_1 \mathbf{S}_2 \cdot \mathbf{q}_2}{\omega_1^2 \omega_2^2}. \quad (3.45b)$$

The contribution from the second term in Eq. (3.44) is included in the pionic current. In the inserted factor,

$$\xi_\Delta(q_1, q_2) = 1 - \frac{f(q_2) - f(q_1)}{q_2^2 - q_1^2} \frac{\omega_1^2}{f(q_1)} - \frac{f_\Delta(q_2) - f_\Delta(q_1)}{q_2^2 - q_1^2} \frac{\omega_2^2}{f_\Delta(q_2)}, \quad (3.46)$$

the pionic current, $\xi_\Delta = 1$, is corrected by the form-factor effect in the πNN and $\pi N \Delta$ vertices.

In Appendix B we present the explicit formula for the partial-wave decomposition of the contact and pionic currents obtained in the static approximation. Our next task is to go beyond the static approximation and evaluate the effects of the retarded pion propagator on the contact and pionic currents. Moreover, in the presence of the pion retardation, the nucleon recoil current brings about a nonvanishing correction.³⁹ In nonstatic calculations we employ the prescription of Aaron, Amado, and Young⁴⁰ for the πNN propagator and the πN relative momentum κ in Eq. (3.36).

IV. RESULTS

The parameters for the πN interaction, the bare mass of Δ , the $\pi N \Delta$ coupling constant and the cutoff momentum, are deduced from the $\pi N P_{33}$ phase shifts. We use model *A* of Ref. 10, the parametrizations of the P_{11} and P_{33} scattering amplitudes. The P_{11} and P_{33} interactions are taken to be rank-two separable, and the πNN and $\pi N \Delta$ form factors are designed to have a common cutoff momentum 1000 MeV/c (dipole). We found that the off-shell behaviors of the πN amplitudes can be represented by the monopole form factor with the cutoff momentum of about 600 MeV/c.

The $\gamma N \Delta$ coupling constant is deduced from the experimental $M_{1+}(\frac{3}{2})$ pion-photoproduction amplitude adopting the πN interaction model in the least-squares fitting. We found that the fitting is insensitive to the cutoff parameter of the background amplitude, and hence we chose 600 MeV/c (monopole). We obtained $f_{\gamma N \Delta} = 3.183$. We show in Fig. 9 the result of our fitting. The background amplitude is also plotted. When we calculate the Δ -isobar current, the background amplitude is subtracted from the full photoproduction amplitude [see Eqs. (2.30) and (2.31)]. The subtraction significantly

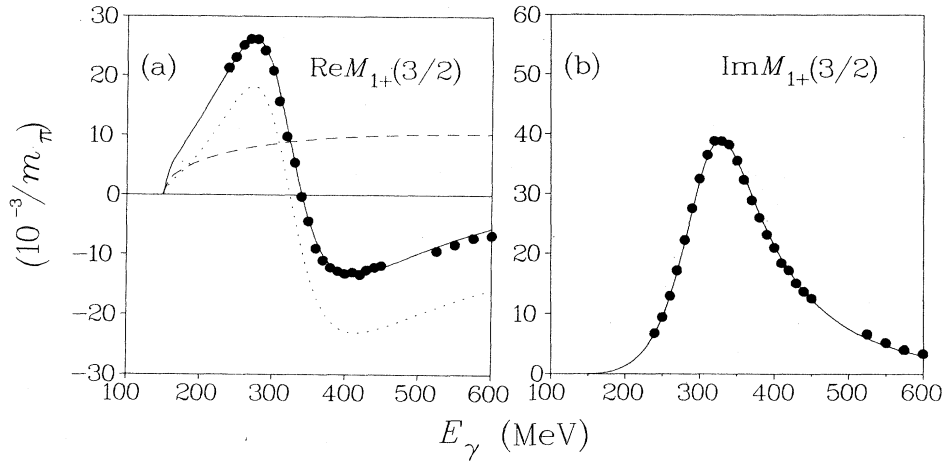


FIG. 9. Fit to the $M_{1+}(\frac{3}{2})$ pion-photoproduction amplitude. The solid curve is the full amplitude, the long-dashed curve is the background, and the short-dashed curve is the full amplitude minus the background. The data are from Ref. 41.

modifies the real part of the amplitude, as is seen in Fig. 9.

Below the pion-production threshold ($E_{\gamma} = 147$ MeV), the normal current with the continuity-equation constraint dominates the deuteron photodisintegration. Arenhövel⁴² showed that above the photon energy $E_{\gamma} \sim 50$ MeV, the magnitude of the amplitude is sensitively influenced by the interaction in the final state. If one neglects the final-state interaction, the total cross section decreases substantially. We observed a similar tendency in our three-body calculation. In Fig. 10 we plot the total cross sections obtained using just the normal current. We compare two different final-state interaction models; the three-body model constructed in our previous paper,¹⁰ and the Paris potential.⁴³ In all these calculations we use the deuteron wave function of the Paris potential.

In Fig. 10 we see that there occur sizable discrepancies between the three-body model and the Paris potential. We investigated the partial-wave amplitudes and found that the major difference is caused by the $E1(^3P_1)$. As is seen in Fig. 11(a), the three-body model does not describe the 3P_1 phase parameters. This is apparently due to our neglect of the short-range interaction. We must admit that our NN elastic amplitude for low partial waves is far from being satisfactory. We decided to use the Paris potential for the final-state interaction in calculating the normal one-body current and the normal one-pion-exchange current. To be consistent with the Paris potential, we follow Buchmann, Leidemann, and Arenhövel⁴⁷ and employ the cutoff momentum 1200 MeV/c (monopole) for the πNN form factor which enters the pion-exchange current. The Δ -isobar current and the Δ one-pion-exchange current are computed using the three-body model. In Fig. 11(b), we see that the three-body model describes satisfactorily the phase parameters of the dominant partial wave 1D_2 .

A. Comparison with Wilhelm, Leidemann, and Arenhövel

We are now in the position to present the results of our full calculations including the normal current, the Δ -isobar current, the one-pion-exchange currents, and the pion reabsorption correction. First we show our predictions using the static approximation given in Sec. III C for the one-pion-exchange currents. In Fig. 12 we exhibit the total cross section. The shape and position of the resonance are quite well reproduced, but its magnitude is slightly underestimated. The experimental peak is located about 50 MeV below the mass of the free $N\Delta$ system. An analogous phenomenon is observed in the $\pi d \rightarrow NN$ reaction. In our previous study,¹¹ we showed that the

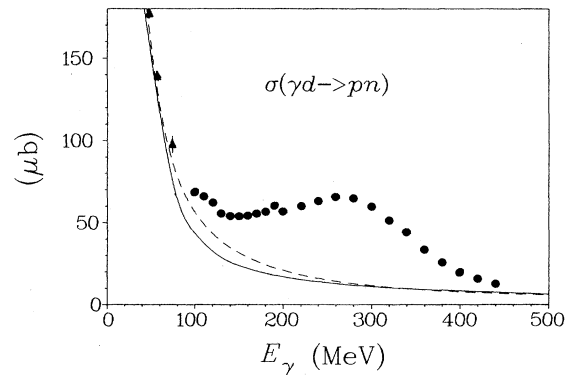


FIG. 10. Contribution of the normal current to the total photodisintegration cross section. The solid and dashed curves give the predictions with the final-state interactions, the three-body model, and the Paris potential, respectively. The data source is as follows: solid triangles from Ref. 44, solid circles from Ref. 45.

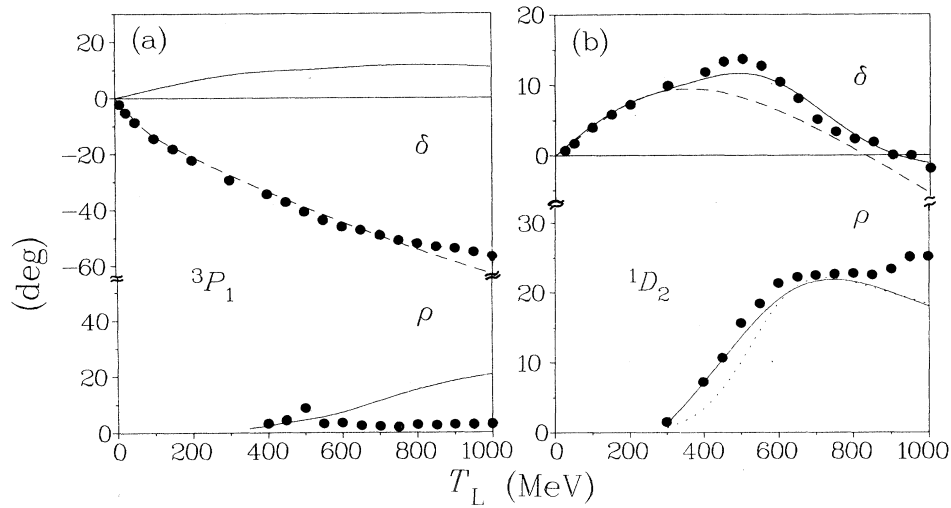


FIG. 11. Energy dependence of the NN scattering phase shifts for the 3P_1 and 1D_2 partial waves. The solid and long-dashed curves are the predictions using the three-body model and the Paris potential, respectively. The inelasticity parameter ρ for the Paris potential is zero. The short-dashed curve is the three-body model prediction with the πd channel coupling ignored. The data are from the analysis of Ref. 46.

final-state interaction shifts the peak of the $\pi d \rightarrow NN$ cross section to a lower energy. In the photodisintegration the perturbative calculations¹³⁻¹⁵ which neglect the final-state interaction bring the maximum of the cross section to higher energies.

At $E_\gamma = 260$ MeV in the vicinity of the maximum of the total cross section, we appreciably underestimate the differential cross section around $\theta_{c.m.} = 90^\circ$. To study the origin of this discrepancy, we compare our result with the coupled-channel calculation of Wilhelm, Leidemann, and Arenhövel¹⁸ in Figs. 13(a) and (b). The most significant difference between these two calculations is seen in the $M1({}^1D_2)$ partial wave which gives the largest contribution in the Δ -resonance region. The model of

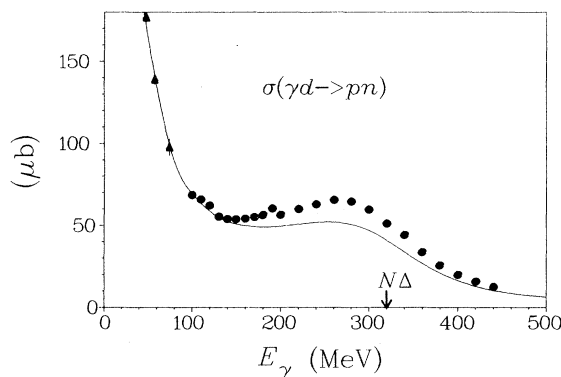


FIG. 12. Energy dependence of the total photodisintegration cross section. The mass of the free $N\Delta$ system is indicated by the arrow. The data are the same as in Fig. 10.

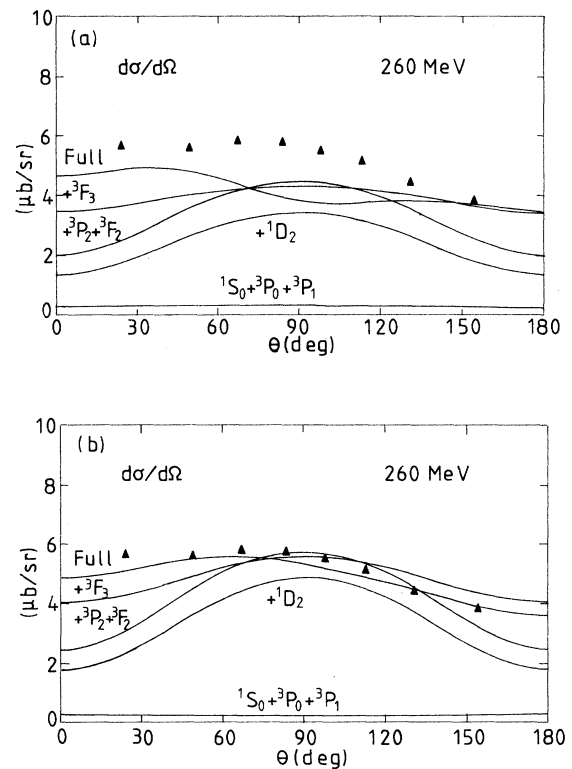


FIG. 13. Partial-wave decomposition of the differential cross section at $E_\gamma = 260$ MeV: (a) the result of the present calculation and (b) that of the coupled-channel model (RSC, 5, V_1) by Wilhelm *et al.*, Ref. 18. The data are from Ref. 48.

TABLE I. Contributions of the normal single-nucleon current, the Δ -isobar current, the normal and Δ -isobar one-pion-exchange currents (OPEC), and the pion-reabsorption process to the $M1(^1D_2)$ amplitude in units of 10^{-3} fm at $E_\gamma = 260$ MeV. In Ref. 18 meson-exchange currents other than OPEC are included. Normalization is as in Ref. 51. The numbers in the parentheses are contributions from the extra current induced by the hadronic form factors at πNN and $\pi N\Delta$ vertices.

	Present	Wilhelm <i>et al.</i> (Ref. 18)
Normal current	$-3.49 - 0.49i$	$-3.37 - 0.34i$
Δ -isobar current	$-5.40 - 7.38i$	$-7.00 - 8.67i$
OPEC	$-1.22 - 0.22i$ ($-0.09 - 0.02i$)	$-1.93 - 0.24i$
Δ -OPEC	$0.00 - 0.09i$ ($0.04 + 0.02i$)	$-0.71 - 0.71i$
Pion reabsorption	$0.19 - 0.23i$	
Total	$-9.92 - 8.41i$	$-13.01 - 9.96i$

Wilhelm *et al.* has freedom in choosing the $\gamma N\Delta$ coupling constant and the $N\Delta \rightarrow NN$ interaction, both of which are essentially important to adjust the total cross section. All of them being considered, their results are better than ours in reproducing the differential cross sections and some polarization parameters. This purports that something is missing in our $M1(^1D_2)$ amplitude.

In Table I we compare the predictions of our model with those of Wilhelm *et al.* by decomposing the dominant $M1(^1D_2)$ partial-wave amplitude. The normal-current contributions agree very well with each other. The results are insensitive to the final-state interaction because the impulse term dominates higher partial waves of the normal current. The essential difference between the two modes is in the Δ -isobar current. Our matrix element is about 20% smaller than Wilhelm *et al.* We also underestimate both the normal and Δ meson-exchange

currents mainly because we did not include the ρ -meson-exchange current nor the $\Delta\Delta$ component of the deuteron wave function. We find that both the effects of the pion reabsorption and the extra additional current induced by the hadronic form factor are negligibly small.

The Δ -isobar current contribution to the $M1(^1D_2)$ amplitude consists of the effective Δ -excitation amplitude and the $N\Delta \rightarrow NN$ transition amplitude. Our results for the NN scattering, Fig. 11(b), and the $\pi d \rightarrow NN$ reaction, Fig. 14, convince us that our model is good enough to adequately describe the $N\Delta \rightarrow NN$ transition. Since the background is subtracted from our $M_{1+}(\frac{3}{2})$ pion-photoproduction amplitude, the real part of the Δ -excitation amplitude is considerably smaller than that of Wilhelm *et al.*, but the imaginary part is much the same.

We also studied the nonstatic effects in the one-pion-exchange currents. In Fig. 15 we show the results for the differential cross sections. The nonstatic propagation in the one-pion-exchange current slightly enhances the cross sections at forward and backward angles, but does not fill in the pronounced dip around $\theta_{c.m.} = 90^\circ$. The results for the neutron and proton polarizations $P_y(n)$, $P_y(p)$, and the photon asymmetry Σ are shown in Figs. 16 and 17. The neutron and proton polarizations are not sensitive to the description of the pion-exchange current. The nonstatic effect in the pion-exchange current most strongly influences the photon asymmetry, but it destroys the good agreement with experiment at low energies.

One more difference between our model and Wilhelm *et al.* is the way the coupling with the πNN and πd channels is introduced. In Wilhelm *et al.* the dominant part of the πNN channel coupling has been taken into account through the width of the Δ . The importance of the πd channel coupling is clearly seen in Fig. 18 in which the partial cross sections of the photon-induced reactions are shown. The cross section for the $\gamma d \rightarrow \pi^0 d$ reaction is about two times larger than the photodisintegration cross section around the mass of the free $N\Delta$ system.

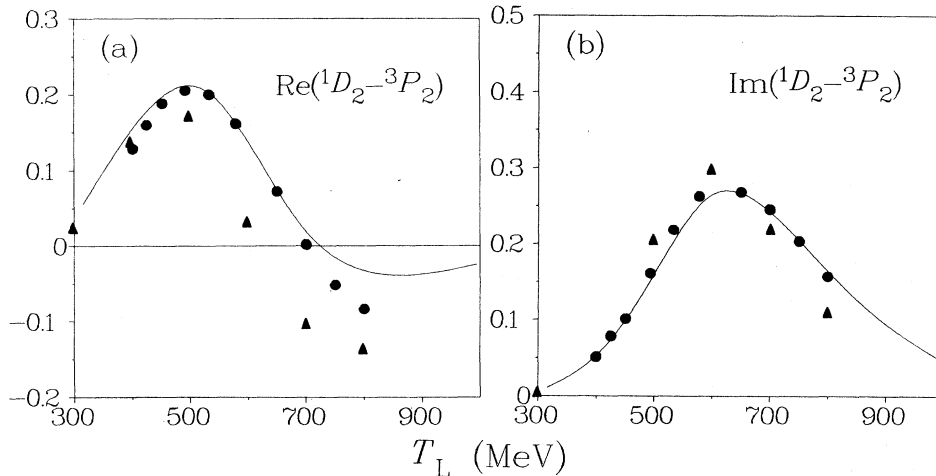


FIG. 14. Prediction for the $NN ^1D_2 - \pi d ^3P_2$ amplitude. The data source is as follows: solid circles from Ref. 49 and solid triangles from Ref. 50.

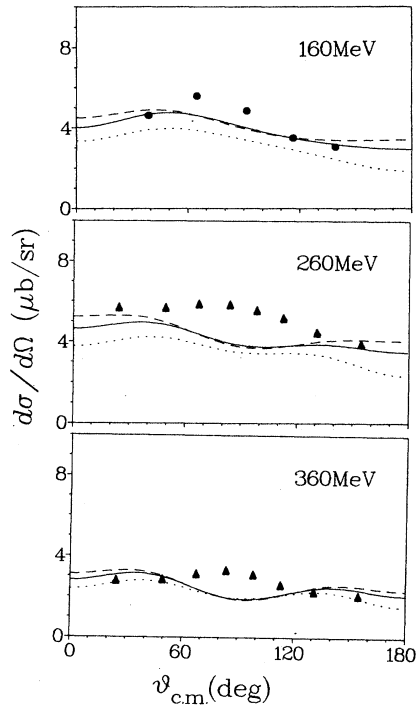


FIG. 15. Angular distributions of the differential cross section at various photon energies. The solid and dashed curves are the results of static and nonstatic calculations of the pion-exchange currents. The dotted curve is the result of the calculation using the three-body model for the final NN interaction. The data source is as follows: solid circles from Ref. 45, solid triangles from Ref. 48.

It is well known⁵⁹ that in the NN inelastic scattering the $NN \rightarrow \pi d$ reaction is the most important process below the nucleon kinetic energy $T_L = 500$ MeV. This is clearly seen in the inelasticity ρ for the 1D_2 partial wave [see Fig. 11(b)]. As Leidemann and Arenhövel¹⁷ neglect the πd channel, they underestimated the inelasticity parameter near the pion-production threshold. In order to reproduce the 1D_2 inelasticity, they introduced a short-range $N\Delta$ interaction with an adjustable parameter. However, it is not possible to simulate the effect of the πd channel coupling by their short-range interaction, because the effective $N\Delta$ interaction arising from the $N\Delta \rightarrow \pi d \rightarrow N\Delta$ transition contains a large imaginary part. In fact, while their short-range interaction enhances the cross section in the Δ -resonance region, the coupling of the πd channel slightly reduces the cross section at $E_\gamma = 300$ MeV, as is shown in Fig. 19.

B. Relativistic corrections

Cambi, Mosconi, and Ricci⁶⁰ pointed out that the spin-orbit correction to the normal current is very important in order to get reasonable results for the forward differential cross section. Wilhelm, Leidemann, and Arenhövel¹⁸ further studied this correction in the Δ -

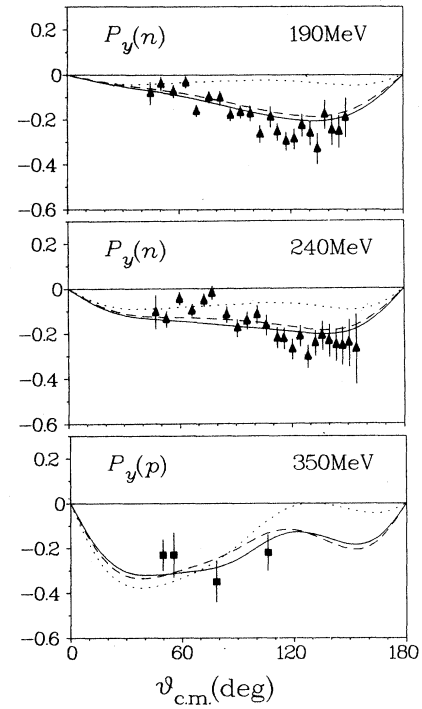


FIG. 16. Angular distributions of the neutron and proton polarizations. Notation is as in Fig. 15. The data source is as follows: solid triangles from Ref. 52, solid squares from Ref. 53.

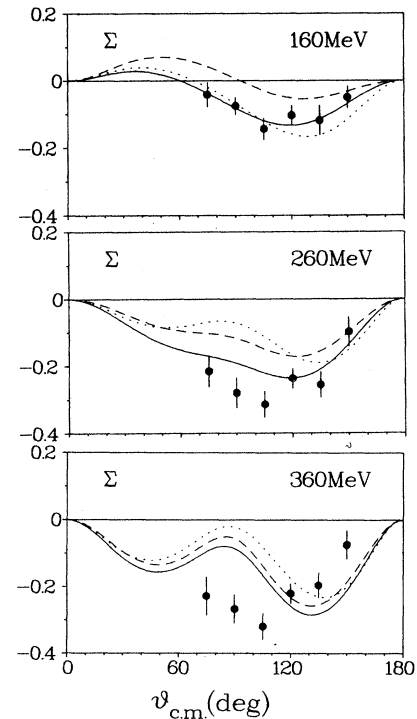


FIG. 17. Angular distributions of the photon asymmetry at various photon energies. Notation is as in Fig. 15. The data are from Ref. 54.

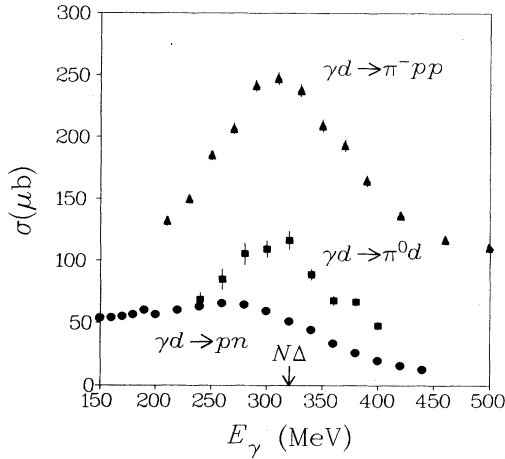


FIG. 18. Total cross sections for the γd reactions. The data source is as follows: solid circles from Ref. 45, solid triangles from Ref. 55, and solid squares from the fits to the data of the differential cross sections, Refs. 56, 57, and 58.

resonance region. They found that the correction is also significant at higher energies.

The spin-orbit term appears in the Foldy-Wouthuysen interaction as a relativistic correction of order m^{-2} . Since the c.m. nucleon momentum reaches as large as 490 MeV at $E_\gamma = 260$ MeV, the effect of terms of higher order in the m^{-1} expansion should be examined in the Δ -resonance region. We calculate the deuteron photodisintegration using the full relativistic interaction given in Sec. III A. The numerical results are shown in Fig. 20. For comparison we also present the nonrelativistic calculation without the spin-orbit correction. The effects of the higher-order terms are found to be very small even in the Δ -resonance region.

The recoil of the Δ also gives rise to the spin-orbit correction to the Δ -isobar current [see Eq. (3.28)]. This does not produce any marked effect below the pion production threshold as is judged from Fig. 20. However, in the Δ -resonance region, it suppresses the differential cross section around $\theta_{c.m.} = 90^\circ$.

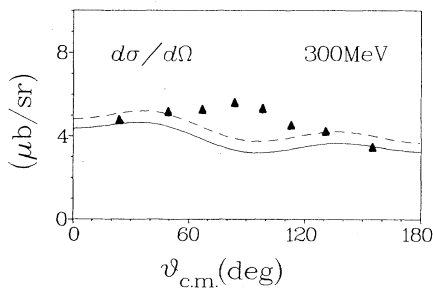


FIG. 19. Effect of the πd channel coupling on the differential cross section at $E_\gamma = 300$ MeV. The full three-body calculation (solid curve) is compared with the calculation without the πd channel coupling (dashed curve).

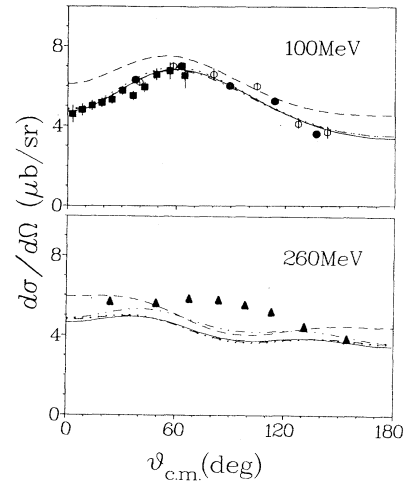


FIG. 20. Effects of the spin-orbit terms and higher-order relativistic corrections on the differential cross sections below and above the pion-production threshold. The solid curve is the calculation to order m^{-2} , the dashed curve is the nonrelativistic calculation, the dot-dashed curve is the result evaluated using the relativistic one-body current, and the dotted curve is the calculation to order m^{-2} but with nonrelativistic kinematics. The double-dot-dashed curve is the calculation without the spin-orbit term in the Δ -isobar current. The data source is as follows: the solid circles from Ref. 45, solid squares from Ref. 61, open circles from Ref. 62, and solid triangles from Ref. 48.

Our model contains another relativistic effect, the Lorentz boost of the pn relative momentum. Figure 20 illustrates the results using the nonrelativistic kinematics: We use relative momentum $\mathbf{Q} = \mathbf{p} + \frac{1}{2}\mathbf{k}$ instead of Eq. (3.26) and ignore the minimal-relativity corrections for both the deuteron wave function and the final-state wave function. The difference between the two calculations is proved to be very small.

C. Generalized Watson's theorem

Below the pion-production threshold Watson's theorem⁶³ demands that the phase of the photodisintegration amplitude should be equal to the final-state NN scattering phase shift δ_l . This constraint is respected in the classic paper by Partovi⁵¹ and in the subsequent papers. Above the pion-production threshold Watson's theorem does not hold true any longer. There occurs deviation of the phase from δ_l . We may write the photodisintegration amplitude as

$$t_l = |t_l| e^{i(\delta_l + \phi_l)}. \quad (4.1)$$

Zukaszuk⁶⁴ proved an inequality for ϕ_l ,

$$\left[\frac{1 - \eta_l}{2} \right]^2 + \eta_l \sin^2 \phi_l \leq \frac{1 - \eta_l^2}{4} \cdot r_l, \quad (4.2)$$

where η_l is the elasticity parameter and

$$r_l = \frac{\sigma_l(\gamma d \rightarrow \pi d, \gamma d \rightarrow \pi NN)}{\sigma_l(\gamma d \rightarrow NN)}. \quad (4.3)$$

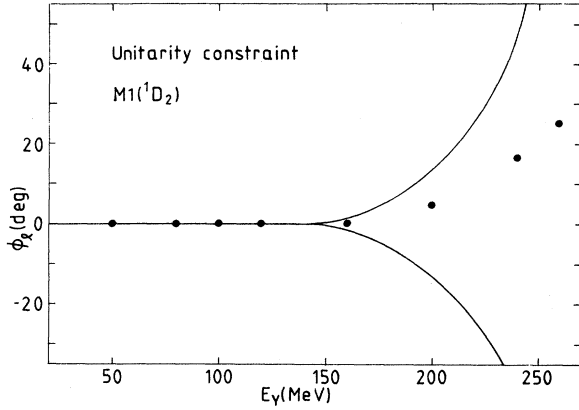


FIG. 21. Unitarity constraint for the phase ϕ_l as a function of the energy. The two curves indicate the upper and lower limits of ϕ_l . The dots are our predictions.

It is easily seen that the inequality is reduced to Watson's theorem ($\phi_l=0$) below the pion-production threshold.

In order to calculate the r_l we need the pion-production cross section for each partial wave. Unfortunately, at present, no such experimental information is available. Alternatively, we estimate roughly the pion-production cross section of the $M1(^1D_2)$ partial wave assuming that it is a sum of the elementary $\gamma p \rightarrow \pi N$ and $\gamma n \rightarrow \pi N$ cross sections in the $M_{1+}(\frac{3}{2})$ partial wave.⁴¹ This estimate is founded on the fact that the $N\Delta$ $^5S_2 \rightarrow NN$ 1D_2 is the largest transition amplitude near the pion-production threshold. The partial waves $E_{0+}(\frac{1}{2})$ and $E_{0+}(\frac{3}{2})$ being non-negligible, their contributions to the $M1(^1D_2)$ amplitude are expected to be very small in the quasifree production.

As shown in Fig. 21, our prediction satisfies Watson's theorem below the pion-production threshold. This is a consequence of the fact that although we have used different final-state interactions for the normal and Δ -isobar currents, both the three-body model and the Paris potential reproduce the phase shift of the 1D_2 partial wave quite well at low energies [see Fig. 11(b)]. Above the pion-production threshold ϕ_l is no longer equal to zero mainly due to the Δ -isobar current. However, it is always within the range of the unitarity constraint.

V. SUMMARY

We have developed a unitary theory of the deuteron photodisintegration. The T matrix consists of the contributions from the normal current, the Δ -isobar current, the one-pion-exchange currents, and the pion-reabsorption correction, all of them being distorted by the final-state interactions. The nonradiative $N\Delta$ - NN transition amplitude is obtained from the coupled equations for the NN - $N\Delta$ - πNN system and is used to describe the final-state interactions of the Δ -mediated currents. On the other hand, the NN - NN amplitude calculated from the Paris potential is used for the normal single-

nucleon and one-pion-exchange currents because the one-pion-exchange force model is unable to describe the NN short-range interaction. Our model is dynamically consistent in the sense that all the parameters are fixed by the πN scattering and single-nucleon pion-photo-production data analyses. We explicitly showed that our photodisintegration amplitude satisfies the unitary constraint.

The gauge invariance is respected at every stage of our calculations. We have used as the single-nucleon current interaction the Dirac electromagnetic interaction that is diagonalized in the positive-energy sector in such a way that the Foldy-Wouthuysen interaction is generalized to all orders in m^{-1} . The continuity-equation constraint is imposed on the normal current and the Δ -isobar current which are not conserved by themselves. In calculating the one-pion-exchange currents, we have included the contributions arising from the πNN and $\pi N\Delta$ vertices as a result of the gauge-invariance constraint.

Our predictions agree very well with the experimental data below the pion-production threshold where the amplitude is dominated by the normal current. In the Δ -resonance region we underestimated the differential cross section around $\theta_{c.m.}=90^\circ$. We confirmed that the spin-orbit term in the normal current suppresses the differential cross section at forward and backward angles. The relativistic corrections of order beyond m^{-2} did not affect the results very much. The extra additional exchange current that arises from the hadronic form factors gave a negligible effect.

ACKNOWLEDGMENTS

One of the authors (H.T.) wishes to thank H. Arenhövel, W. Leidemann, and P. Wilhelm for many helpful discussions and for providing him with the results of their calculations. His work was supported by the Deutsche Forschungsgemeinschaft (SFB201).

APPENDIX A: PARTIAL-WAVE EXPANSION OF THE ONE-BODY CURRENTS

The magnetic and Coulomb multipoles are decomposed as

$$\begin{aligned}
 M_L(l_s J) = & g_1 \hat{L} W_{LLl_s J}^{101} + g_3 \hat{L} W_{LLl_s J}^{111} \\
 & + g_4 (\sqrt{L+1} W_{LL-1l_s J}^{011} + \sqrt{L} W_{LL+1l_s J}^{011}) \\
 & + g_5 (\sqrt{L+1} W_{LL-1l_s J}^{211} + \sqrt{L} W_{LL+1l_s J}^{211}), \quad (A1)
 \end{aligned}$$

$$\begin{aligned}
 C_L(l_s J) = & h_1 \hat{L} W_{LLl_s J}^{000} \\
 & + h_2 (\sqrt{L} W_{LL-1l_s J}^{111} - \sqrt{L+1} W_{LL+1l_s J}^{111}), \quad (A2)
 \end{aligned}$$

where we have used the notation $\hat{L} = \sqrt{2L+1}$. The electric multipole is calculated from Eq. (3.6) using the Coulomb multipole and

$$\begin{aligned} \hat{L}J_{LL+1}(lsJ) &= g_1 \hat{L}W_{LL+1lsJ}^{101} - g_2 \sqrt{L+1} W_{LLlsJ}^{000} \\ &+ g_3 \hat{L}W_{LL+1lsJ}^{111} + g_4 \sqrt{L} W_{LLlsJ}^{011} \\ &+ g_5 \sqrt{L} W_{LLlsJ}^{211}. \end{aligned} \quad (\text{A3})$$

The reduced matrix elements W are defined by

$$\begin{aligned} W_{Ll_0lsJ}^{l_p rc} &= \langle lsJ || [C_{l_p}(\hat{p}) \times \sigma^{(r)}]_c \phi(\mathbf{Q}) || Ll_0J \rangle \\ &= \sum_{L_d, a, \Lambda} S^{L_d a \Lambda} A^{L_d a \Lambda}. \end{aligned} \quad (\text{A4})$$

The spin part is given by

$$\begin{aligned} S^{L_d a \Lambda} &= (-)^P \hat{s}_2 \hat{c} \hat{L}_d \hat{S}_d \hat{j}_d \hat{L} \hat{l}_0 \hat{l} \hat{s} \hat{\Lambda}^2 \left[\frac{(2L_d+1)!}{(2a)!(2L_d-2a)!} \right]^{1/2} \langle s_2 || \sigma^{(r)} || \frac{1}{2} \rangle \begin{Bmatrix} r & S_d & s \\ \frac{1}{2} & s_2 & \frac{1}{2} \end{Bmatrix} \begin{Bmatrix} l_0 & a & \Lambda \\ 0 & 0 & 0 \end{Bmatrix} \\ &\times \sum_b \hat{b}^2 \begin{Bmatrix} l_p & l & b \\ 0 & 0 & 0 \end{Bmatrix} \begin{Bmatrix} L_d - a & b & \Lambda \\ 0 & 0 & 0 \end{Bmatrix} \begin{Bmatrix} a & L_d - a & L_d \\ b & l_0 & \Lambda \end{Bmatrix} \begin{Bmatrix} l_p & l & b & L_d \\ r & s & S_d & L \\ c & J & l_0 & j_d \end{Bmatrix}, \end{aligned} \quad (\text{A5})$$

where L_d, S_d, j_d are the deuteron quantum numbers, s_2 is the spin of the nucleon (the normal current) or Δ (the Δ -isobar current),

$$P = J + j_d + s + L + \Lambda + l_p + r + 1, \quad (\text{A6})$$

and

$$\langle s || \sigma^{(r)} || \frac{1}{2} \rangle = \begin{cases} 1 & \text{for } s = \frac{1}{2} \text{ and } r = 0 \\ \sqrt{3} & \text{for } s = \frac{1}{2} \text{ and } r = 1 \\ 1 & \text{for } s = \frac{3}{2} \text{ and } r = 1 \end{cases} \quad (\text{A7})$$

The radial part is given by

$$A^{L_d a \Lambda} = \sqrt{4\pi p} L_d^{-a} k^{\frac{a-1}{2}} \int_{-1}^1 dx P_\Lambda(x) \beta^a \frac{\phi_{L_d}(Q)}{Q^{L_d}}, \quad (\text{A8})$$

where the integration is over $x = \hat{p} \cdot \hat{k}$, $\phi_{L_d}(Q)$ is the radial part of the deuteron wave function in momentum space, and $\mathbf{Q} = \mathbf{p} + \beta \mathbf{k}$, where $\beta = \frac{1}{2}$ in the nonrelativistic limit. A factor of $2\sqrt{2}$ is to be multiplied for the normal current, and 2 for the Δ -isobar current. We take into ac-

count the weakly x -dependent form factors by including them into the integrand.

APPENDIX B: PARTIAL-WAVE EXPANSION OF THE TWO-BODY CURRENTS

The contact current is expanded in partial waves

$$J_{Ll_0}(lsJ) = \sum_{L_d, a, \Lambda} \mathcal{S}_1 A_{l_0, 1}^{L_d a \Lambda} + \frac{k}{2} \sum_{L_d, a, \Lambda, K} \mathcal{S}_2 A_{K, 0}^{L_d a \Lambda}. \quad (\text{B1})$$

The spin part is given by

$$\mathcal{S}_1 = \sum_K \mathcal{S}_2, \quad (\text{B2})$$

$$\begin{aligned} \mathcal{S}_2 &= (-1)^L \hat{K}^2 \begin{Bmatrix} K & 1 & l_0 \\ 0 & 0 & 0 \end{Bmatrix} \\ &\times \sum_d \hat{d}^2 \begin{Bmatrix} K & 1 & l_0 \\ 1 & L & d \end{Bmatrix} S_{dK}^{L_d a \Lambda}, \end{aligned} \quad (\text{B3})$$

where

$$\begin{aligned} S_{de}^{L_d a \Lambda} &= (-)^P \hat{s}_1 \hat{s}_2 \hat{L}_d \hat{S}_d \hat{j}_d \hat{L} \hat{l}_0 \hat{l} \hat{s} \hat{\Lambda}^2 \left[\frac{(2L_d+1)!}{(2a)!(2L_d-2a)!} \right]^{1/2} \langle s_1 || \sigma^{(1)} || \frac{1}{2} \rangle \langle s_2 || \sigma^{(1)} || \frac{1}{2} \rangle \begin{Bmatrix} s_1 & \frac{1}{2} & 1 \\ s_2 & \frac{1}{2} & 1 \\ s & S_d & d \end{Bmatrix} \\ &\times \begin{Bmatrix} e & a & \Lambda \\ 0 & 0 & 0 \end{Bmatrix} \begin{Bmatrix} L_d - a & l & \Lambda \\ 0 & 0 & 0 \end{Bmatrix} \begin{Bmatrix} a & L_d - a & L_d \\ l & e & \Lambda \end{Bmatrix} \begin{Bmatrix} l & L_d & e \\ s & S_d & d \\ j & j_d & L \end{Bmatrix}, \end{aligned} \quad (\text{B4})$$

s_1 and s_2 are the spins of N or Δ , and

$$P = J + j_d + L + \Lambda + l + d + 1, \quad (\text{B5})$$

The radial part is given by

$$A_{K, n}^{L_d a \Lambda} = (4\pi)^{3/2} p^{L_d - a} \int_0^\infty q^2 dq q^{n+a} F_K(q, k) G_\Lambda(q, p), \quad (\text{B6})$$

where

$$F_K(q, k) = \frac{1}{2} \int_{-1}^1 dx P_K(x) \frac{f_1(q_2) f_2(q_2)}{\omega_2^2}, \quad (\text{B7})$$

$$G_{\Lambda}(q,p) = \frac{1}{2} \int_{-1}^1 dx P_{\Lambda}(x) \frac{\phi_{L_d}(|\mathbf{p}+\mathbf{q}|)}{|\mathbf{p}+\mathbf{q}|^{L_d}}. \quad (\text{B8})$$

The form factors f_1 and f_2 are either the πNN or $\pi N\Delta$ vertex function. We have made a change of variables such that $\mathbf{q}_1 = \mathbf{q} - \frac{1}{2}\mathbf{k}$ and $\mathbf{q}_2 = \mathbf{q} + \frac{1}{2}\mathbf{k}$. The integration is over $x = \hat{\mathbf{q}} \cdot \hat{\mathbf{k}}$ for $F_K(q,k)$ and over $x = \hat{\mathbf{q}} \cdot \hat{\mathbf{p}}$ for $G_{\Lambda}(q,p)$. A factor 2 is necessary due to the existence of two identical processes.

In the same way the pionic current becomes

$$J_{L_0}(lsJ) = \sum_{L_d, a, \Lambda} \mathcal{S}_1 A_{l_0, 3}^{L_d a \Lambda} + \frac{k}{2} \sum_{L_d, a, \Lambda, K} \mathcal{S}_2 A_{K, 2}^{L_d a \Lambda} + \frac{k^2}{4} \sum_{L_d, a, \Lambda, K} \mathcal{S}_3 A_{K, 1}^{L_d a \Lambda}, \quad (\text{B9})$$

where

$$\mathcal{S}_1 = \begin{bmatrix} l_0 & 1 & L \\ 0 & 0 & 0 \end{bmatrix} \sum_{d,e} \hat{d}^2 \hat{e}^2 \begin{bmatrix} 1 & 1 & d \\ 0 & 0 & 0 \end{bmatrix} \begin{bmatrix} e & d & L \\ 0 & 0 & 0 \end{bmatrix} S_{de}^{L_d a \Lambda}, \quad (\text{B10})$$

$$\mathcal{S}_2 = \hat{K}^2 \begin{bmatrix} K & 1 & l_0 \\ 0 & 0 & 0 \end{bmatrix} \sum_{d,e} \hat{d}^2 \hat{e}^2 [1 - (-)^d] S_{de}^{L_d a \Lambda} \sum_f \hat{f}^2 \begin{bmatrix} f & 1 & 1 \\ 0 & 0 & 0 \end{bmatrix} \begin{bmatrix} K & f & e \\ 0 & 0 & 0 \end{bmatrix} \begin{bmatrix} K & 1 & l_0 \\ f & 1 & 1 \\ e & d & L \end{bmatrix}, \quad (\text{B11})$$

$$\mathcal{S}_3 = \hat{K}^2 \sum_{d,e} \hat{d}^2 \hat{e}^2 \begin{bmatrix} 1 & 1 & d \\ 0 & 0 & 0 \end{bmatrix} \begin{bmatrix} e & 1 & K \\ 0 & 0 & 0 \end{bmatrix} \begin{bmatrix} l_0 & d & K \\ 0 & 0 & 0 \end{bmatrix} \begin{bmatrix} e & d & L \\ l_0 & 1 & K \end{bmatrix} S_{de}^{L_d a \Lambda}. \quad (\text{B12})$$

$F_K(q,k)$ should be replaced by

$$F_K(q,k) = \frac{1}{2} \int_{-1}^1 dx P_K(x) \xi(q_1, q_2) \frac{2f_1(q_1)f_2(q_2)}{\omega_1^2 \omega_2^2}. \quad (\text{B13})$$

For the $d \rightarrow N\Delta$ pionic current, an additional factor 2 is necessary because the Δ is excited from either of the two nucleons. For all the $d \rightarrow NN$ two-body currents, a factor $\sqrt{2}$ is necessary from antisymmetrization. The trivial isospin matrix element is not written down.

- ¹I. R. Afnan and A. W. Thomas, Phys. Rev. C **10**, 107 (1974).
²B. Blankleider and I. R. Afnan, Phys. Rev. C **24**, 1572 (1981).
³T. Mizutani, C. Fayard, G. H. Lamot, and R. S. Nahabetian, Phys. Lett. **107B**, 177 (1981).
⁴A. S. Rinat and Y. Starkand, Nucl. Phys. **A397**, 381 (1983).
⁵W. M. Kloet and R. R. Silbar, Nucl. Phys. **A338**, 281 (1980).
⁶J. Dubach, W. M. Kloet, A. Cass, and R. R. Silbar, Phys. Lett. **106B**, 29 (1981).
⁷A. Matsuyama and K. Yazaki, Nucl. Phys. **A364**, 477 (1981).
⁸T. Ueda, Phys. Lett. **141B**, 157 (1984).
⁹H. Garcilazo, Phys. Rev. C **35**, 1820 (1987).
¹⁰H. Tanabe and K. Ohta, Phys. Rev. Lett. **56**, 2785 (1986); Nucl. Phys. **A484**, 493 (1988).
¹¹H. Tanabe and K. Ohta, Phys. Rev. C **36**, 2495 (1987).
¹²N. Austern, Phys. Rev. **100**, 1522 (1955); F. Zachariassen, *ibid.* **101**, 371 (1956); R. R. Wilson, *ibid.* **104**, 218 (1956).
¹³J. M. Laget, Nucl. Phys. **A312**, 265 (1978); Phys. Rep. **69**, 1 (1981).
¹⁴K. Ogawa, T. Kamae, and K. Nakamura, Nucl. Phys. **A340**, 451 (1980).
¹⁵M. Anastasio and M. Chemtob, Nucl. Phys. **A364**, 219 (1981).
¹⁶W.-Y. Hwang and G. E. Walker, Ann. Phys. (N.Y.) **159**, 118 (1985).
¹⁷W. Leidemann and H. Arenhövel, Nucl. Phys. **A465**, 573 (1987).
¹⁸P. Wilhelm, W. Leidemann, and H. Arenhövel, Few-Body Systems **3**, 111 (1988).
¹⁹P. U. Sauer, Few-Body Systems Suppl. **2**, 215 (1987).

- ²⁰M. Araki and I. R. Afnan, Phys. Rev. C **38**, 213 (1988).
²¹M. G. Olsson, Nucl. Phys. **B78**, 55 (1974).
²²C. Lovelace, Phys. Rev. **135**, B1225 (1964).
²³J. H. Koch and E. J. Moniz, Phys. Rev. C **27**, 751 (1983); J. H. Koch, E. J. Moniz, and N. Ohtsuka, Ann. Phys. (N.Y.) **154**, 99 (1984).
²⁴H. Tanabe and K. Ohta, Phys. Rev. C **31**, 1876 (1985).
²⁵G. E. Brown, A. D. Jackson, and T. T. S. Kuo, Nucl. Phys. **133**, 481 (1969).
²⁶J. M. Eisenberg and W. Greiner, *Nuclear Theory* (North-Holland, Amsterdam, 1970), Vol. II.
²⁷I. T. Cheon, Suppl. Prog. Theor. Phys. Extra Number, 146 (1968); M. V. Barnhill, Nucl. Phys. **A131**, 106 (1969).
²⁸E. Eriksen and M. Kolsrud, Nuovo Cimento Suppl. **18**, 1 (1960).
²⁹K. Ohta, J. Phys. A **20**, 389 (1987); J. Phys. G **14**, 449 (1988).
³⁰K. Ohta and M. Ichimura, Nucl. Phys. **A491**, 509 (1989).
³¹If one prefers no unitary transformation ($S=0$), $u(-\mathbf{p})^{\dagger}u(-\mathbf{p}-\mathbf{k})$ appears in the right-hand side of Eq. (3.18). See Ref. 30.
³²L. L. Foldy and S. A. Wouthuysen, Phys. Rev. **78**, 29 (1950).
³³A. Cambi, B. Mosconi, and P. Ricchi, J. Phys. G **10**, L11 (1984).
³⁴We use the pseudoscalar πN interaction so that the contact amplitude arises from nucleon-antinucleon pair excitation. This does not necessarily mean that the $N\bar{N}$ excitation is a physical process. Considering the compositeness of the nucleon, it is quite likely that the pair creation is suppressed at

- the low-energy regime, and yet the use of the pseudoscalar theory is not completely wrong since the contact interaction is predominated by the model-independent Kroll-Ruderman term. See Ref. 30. From the practical point of view, the contact-term contribution to the $M_{1+}(\frac{3}{2})$ amplitude is very small.
- ³⁵L. Heller, S. Kumano, J. C. Martinez, and E. J. Moniz, *Phys. Rev. C* **35**, 718 (1987).
- ³⁶K. Ohta, *Nucl. Phys.* **A495**, 564 (1989).
- ³⁷M. A. Maize and Y. E. Kim, *Nucl. Phys.* **A420**, 365 (1984).
- ³⁸F. Gross and D. O. Riska, *Phys. Rev. C* **36**, 1928 (1987).
- ³⁹J. L. Friar, *Ann. Phys. (N.Y.)* **104**, 380 (1977).
- ⁴⁰R. Aaron, R. D. Amado, and J. E. Young, *Phys. Rev.* **174**, 2022 (1968).
- ⁴¹F. A. Berends and A. Donnachie, *Nucl. Phys.* **B84**, 342 (1975); **B136**, 317 (1978).
- ⁴²H. Arenhövel, *Z. Phys. A* **302**, 25 (1981).
- ⁴³M. Lacombe *et al.*, *Phys. Rev. D* **21**, 861 (1980).
- ⁴⁴R. Bernabei *et al.*, *Phys. Rev. Lett.* **57**, 1452 (1986).
- ⁴⁵E. De Sanctis *et al.*, *Phys. Rev. C* **34**, 413 (1986).
- ⁴⁶R. A. Arndt, J. S. Hyslop III, and L. D. Roper, *Phys. Rev. D* **35**, 128 (1987).
- ⁴⁷A. Buchmann, W. Leidemann, and H. Arenhövel, *Nucl. Phys.* **A443**, 726 (1985).
- ⁴⁸J. Arends *et al.*, *Nucl. Phys.* **A412**, 509 (1984).
- ⁴⁹D. V. Bugg, A. Hasan, and R. L. Shypit, *Nucl. Phys.* **A477**, 546 (1988).
- ⁵⁰N. Hiroshige, W. Watari, and M. Yonezawa, *Prog. Theor. Phys.* **72**, 1146 (1984).
- ⁵¹F. Partovi, *Ann. Phys. (N.Y.)* **27**, 74 (1964).
- ⁵²H. Hugi *et al.*, *Nucl. Phys.* **A472**, 701 (1987).
- ⁵³F. F. Liu *et al.*, *Phys. Rev.* **165**, 1478 (1968).
- ⁵⁴V. G. Gorbenko *et al.*, *Nucl. Phys.* **A381**, 330 (1982).
- ⁵⁵P. Benz *et al.*, *Nucl. Phys.* **B15**, 158 (1973).
- ⁵⁶G. van Holtey *et al.*, *Z. Phys.* **259**, 51 (1973).
- ⁵⁷B. Bouquet *et al.*, *Nucl. Phys.* **B79**, 45 (1974).
- ⁵⁸E. Hilger *et al.*, *Nucl. Phys.* **B93**, 7 (1975).
- ⁵⁹B. J. VerWest and R. A. Arndt, *Phys. Rev. C* **25**, 1979 (1982).
- ⁶⁰A. Cambi, B. Mosconi, and P. Ricci, *Phys. Rev. Lett.* **48**, 462 (1982).
- ⁶¹H. O. Meyer *et al.*, *Phys. Rev. C* **31**, 309 (1985).
- ⁶²J. M. Cameron *et al.*, *Nucl. Phys.* **A458**, 637 (1986).
- ⁶³K. M. Watson, *Phys. Rev.* **95**, 228 (1954).
- ⁶⁴L. Łukaszuk, *Phys. Lett.* **47B**, 51 (1973).